Scientific Journal of Silesian University of Technology. Series Transport
Zeszyty Naukowe Politechniki Śląskiej. Seria Transport

Volume 130 **2026**

p-ISSN: 0209-3324

e-ISSN: 2450-1549

DOI: https://doi.org/10.20858/sjsutst.2026.130.1

Journal homepage: http://sjsutst.polsl.pl

Article citation information:
Aremu, O.O., Adeyemi, A., Oke, S.A., Ola, I.A. Simulation of basic factors affecting the exhaust gas recirculation system as a means of emission control in a spark ignition engine. *Scientific Journal of Silesian University of Technology. Series Transport*. 2026, **130**, 5-40. ISSN: 0209-3324. DOI: https://doi.org/10.20858/sjsutst.2026.130.1

Olaniyi Olateju AREMU[1], Adeyinka ADEYEMI[2], Sunday Ayoola OKE[3], Ibukun Adekola OLA[4]

SIMULATION OF BASIC FACTORS AFFECTING THE EXHAUST GAS RECIRCULATION SYSTEM AS A MEANS OF EMISSION CONTROL IN A SPARK IGNITION ENGINE

Summary. In spark ignition engines, engine performance and emission control are determined through the varying influence of exhaust gas recirculation and its aero-dynamic properties. However, few intensive studies are available in this domain. This paper simulates the combustion process in a spark ignition engine, studying the effects of exhaust gas recirculation (EGR) control mechanism on engine performance parameters and the aerodynamic properties of the EGR value, for optimum emission control. Thermodynamic engine models were used for the simulation of the combustion process. Cycle peak temperature reduction was used to assess the EGR system in the emission control of NOx. Hence, the simulation was structured to yield the volume, temperature and pressure of the engine cylinder, every degree crank angle at varying% EGR (say 0 to 20% of recycled exhaust gas). The effect of% EGR on indicated power, indicated thermal efficiency, indicated

[1] Department of Design and Development, Federal Institute of Industrial Research, Oshodi, Lagos. Email: aremuolateju@yahoo.com. ORCID: https://orcid.org/0009-0000-6481-4968
[2] Department of Mechanical Engineering, University of Lagos, University Road, Akoka, Yaba, Lagos, Nigeria. Email: saoke01@gmail.com. ORCID: https://orcid.org/0009-0007-0303-6171
[3] Department of Mechanical Engineering, University of Lagos, University Road, Akoka, Yaba, Lagos, Nigeria. Email: sa_oke@yahoo.com. ORCID: https://orcid.org/0000-0002-0914-8146
[4] Department of Agricultural and Bio-resource Engineering, College of Engineering, Federal University of Agriculture Abeokuta Nigeria. Email: olaia@funaab.edu.ng. ORCID: https://orcid.org/0000-0003-2825-8700

mean effective pressure, cycle peak temperature and cycle peak pressure were simulated. Aero dynamic properties of the EGR value were simulated to examine the factors that affect the EGR value in metering the required quantity of recycled exhaust gas into the engine intake. The effect of temperature, velocity, pressure and area of flow of the EGR gas through the EGR value were simulated. BASIC program was written to generate simulated data, which were plotted with Microsoft Excel. The principal results of this study include a reduction in the net work done by the engine (0.393 kJ at 0% EGR to 0.353 kJ at 20% EGR) as the recycled exhaust gas increases. Moreover, an inverse variation between the indicated power and% EGR existed (5.895 kW at% EGR to 5.290 kW at 20% EGR). Furthermore, an inverse variation between the cylinder peak pressure and% EGR was observed (5681 kPa at 0% EGR to 5228 kPa at 20% EGR). Overall, significant control of the emission of NOx was achieved through the use of the EGR, system, demonstrating the robustness of the proposed framework.

Keywords: emission, engines, thermal efficiency, spark engine, combustion

1. INTRODUCTION

At present, there is a huge but progressive demand from users for highly efficient but also ecologically-sound spark ignition (SI) engines [1]. This challenge researchers in search for advanced methods and ideas to optimize engine performance by modifying combustion and controlling emissions from the process [1]. One such idea is the use of exhaust gas recirculation (EGR), is capable of improving engine efficiency, reducing NOx emissions, minimizing fuel consumption and improving combustion [2, 3]. Moreover, EGR can provide useful and reliable estimates of the effects of its variations on the diverse engine parameters in a spark ignition engine. Notwithstanding the wide appeal of the EGR concept and its crucial function in drastically reducing emissions, improving efficiency and fuel consumption in several areas of commerce and engineering, it has faced limited research. Extensive studies on the effects of variations of the EGR on the key parameters of the SI engine are hardly found in the literature.

Moreover, the exhaust gas recirculation system is one of the several methods being used in the emission control of exhaust gases. Exhaust Gas Recirculation (EGR) system involves dilution of the intake charge with some quantity of exhaust gas (say 10% or less) so as to reduce the temperature of the combustion chamber [4]. EGR is mostly used to control the emission of oxides of nitrogen. An EGR system requires the use of a specially built EGR valve, which opens a passage between the exhaust and the intake manifold. A typical EGR valve is a vacuum-operated valve, and various types of EGR control systems include: Temperature control, Backpressure transducer, Ported vacuum control, and electrically controlled solenoid valve. An EGR valve simply regulates and times the recycled exhaust gas flow.

The scope of this research was to cover only Spark Ignition (SI) engines. It has been observed that SI engines and diesel engines largely contribute to urban pollution. Exhaust gases from SI engine contain the following pollutants: Carbon-monoxide (CO), hydrocarbons (HC), nitric oxides (NO), and nitrogen dioxide (NO_2). NO and NO_2 are collectively referred to as NOx, i.e. oxides of nitrogen. Simulation of an emission control system using EGR requires an iterative analysis which predicts the quantity of the recycled exhaust gas and ensures that the recycled exhaust gas does not deteriorate the combustion process beyond certain limits. Continuing efforts to enhance the thermal efficiency of the SI engine while simultaneously reducing its undesirable exhaust emissions have resulted in close attention being focused on

a total understanding of the combustion process. Therefore, simulation of some basic factors that affect the EGR system in emission control is of great importance as it would help engine developers in optimizing engine geometries and the EGR valve, early in the design process. In this work, some applicable SI engine models were used, and a BASIC computer program was written to predict the peak combustion temperature for each cycle. The program also gives the percentage of the recycled exhaust gas to dilute the intake charge in order to achieve a minimum NO_x pollution. Aerodynamic properties of the EGR valve were also considered.

2. LITERATURE REVIEW

Several studies on SI engines and the application of EGR for its emission control had been carried out by some researchers, some of whom are referenced in this report.

Tahtouh et al. [5] examined the PHOENICE engine by targeting to attain lean combustion, moderate-pressure exhaust gas recirculation, and towering compression ratio. Two principal contributions were announced: (1) the attainment of 45% as the peak indicated thermal efficiency and reduced brake specific fuel consumption (by 10%).[6] studied a spark ignition engine and concluded that an accurate performance assessment of the engine parameters was possible. Aderibigbe et al. [1] presented a predictive artificial neural network model for engine performance measurement with a focus on the SI engine. It was ascertained that the most efficient architecture is the 6-13-9-6-8 network. The 28 neurons in three hidden layers showed tremendous predictive ability in the spark ignition engine experiment. Lee et al. [2] compared the dual and single- spark ignition systems on the basis of the influence of ignition on the combustion scheme, given the condition at 1600 rpm/gIMEP 0.7MPa. It was reported that for the dual-spark ignition, the net indicated average effective pressure to be 2.71% given the excessive air proposition of 155 condition, which exceeded the single-spark ignition by 5%.

Paluch et al. [3] established the influence of hydrogen when added to the air-fuel addition that was connected to a spark-ignition engine. It was reported that on the basis of utility and ecology, hydrogen served as an adequate fuel additive for the traditional spark ignition engine [7]. Assad et al. [8] conducted an analysis on 16 hydrocarbon classes emitted by a spark-ignition engine by deploying the spectroscopy method. It was concluded that the emission of hydrocarbons when the engine was operated via the principal avenues of vehicle operation is multiple times above the established values for atmospheric air pollution by the European Agency for Atmospheric Air and the World Health Organization [9].

Sforza et al. [10] analyzed a spark ignition engine by focusing on a one-dimensional and three-dimensional study where the engine is fed with premixed [11] theoretically examined the properties of spark ignition engines operated within the Nigerian environment. All performance parameters showed increases as the engine load increased.

3. THEORETICAL MODELLING

3.1 Simulation of combustion process

The following theoretical models were used to simulate the cylinder pressure and temperature of an SI engine (Figure 1). The combustion process is assumed to take place within a closed system with no loss of in-cylinder gas due to blowby gases. The gases within the cylinder were also assumed to be ideal. It was also assumed that there was uniform

temperature in the whole mass within the cylinder at any crank angle degree (i.e. one-zone model.)

Applying the first law of thermodynamics to the gas within the cylinder when the inlet and exhaust valves are closed gives the following:

$$\frac{dQ}{d\theta} - \frac{PdV}{d\theta} = m\frac{dE}{d\theta} \tag{1}$$

$$PV = mRT \tag{2}$$

The heat released due to the combustion of fuel consists of Apparent Heat released and Convective Heat loss. These are shown in equation (3) as follows:

$$(^{dQ}/_{d\theta}) = (^{dQ}/_{d\theta})_{app} + HA(T_{wall} - T)/(^{dQ}/_{dt}) \tag{3}$$

The Convective heat transfer coefficient, H, was estimated using the Eichelberg Model [12]:

$$H = 2.466 \times 10^{-4}((S)(N)/30)^{1/3}(PT)^{1/2} \tag{4}$$

To change the unit of H from KW/m^2 ^{o}K to KJ/ m^2 ^{o}Kdeg , divide the above H in eqn (4) with 6N where N is in rev/min. (i.e. $(^{dt}/_{d\theta}) = 1/(6N)$).

The Blumberg Model was used for the estimation of the Apparent Heat released rate. It is as follows:

$$(^{dQ}/_{d\theta})_{app} = \frac{(LHV)(m_{af})(FA)}{2\,(\theta_C)\,(1 + FA)} \left\{\mathrm{Sin}(^{p(\theta - \theta o)}/_{\theta_c})\right\} \tag{5}$$

The Blumberg model assumed that the apparent heat release rate and mass burned fraction are a trigonometric function of the crank angle [12].

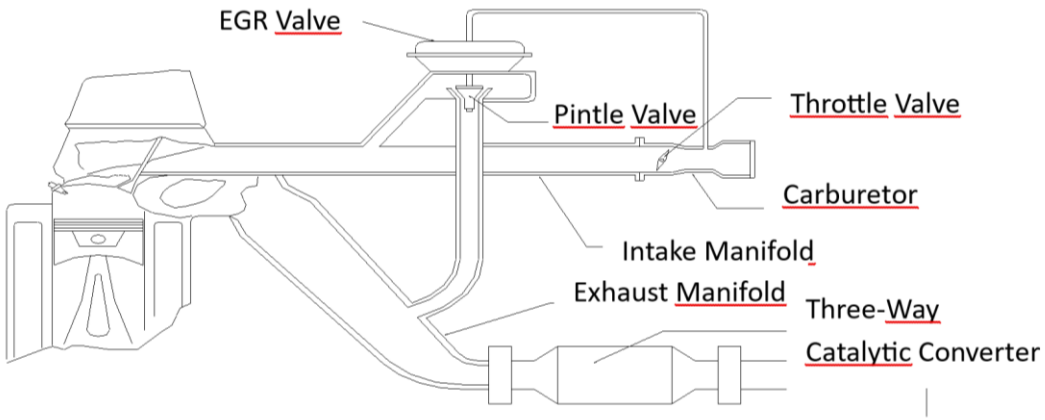

Fig.1. Physical model of a four-stroke SI engine showing the use of the EGR valve in emission control

The heat transfer area, A_{con}, was found assuming the combustion chamber is cylindrical in construction and is calculated as follows:

$$A_{con} = \pi B\{x + B/2 + 4V_c/\pi B^2\} \quad (6)$$

Piston displacement, x, which is the distance measured from the piston head to TDC, is calculated using the crank-slider equation [13]:

$$x = l + r(1 - \cos\theta) - \sqrt{(l^2 - r^2\sin^2\theta)} \quad (7)$$

Instantaneous cylinder volume, V_θ, at any degree crank angle θ is calculated as follows: (assuming that the piston head surface is flat.)

$$V_\theta = V_s/(CR - 1) + (\pi B^2/4)\left\{1 + r(1 - \cos\theta) - \sqrt{(l^2 - r^2\sin^2\theta)}\right\} \quad (8)$$

Derivative of the cylinder volume with respect to crank angle is given by the equation (9)

$$(^{dV}/_{d\theta}) = (\pi B^2/4)\, r \sin\theta\left\{1 - r\cos\theta/\sqrt{(l^2 - r^2\sin^2\theta)}\right\} \quad (9)$$

Combining equations (1), (2) and (3) above, and assuming that specific heats are constant; then we have:

$$(^{dP}/_{d\theta}) = \left\{ (^{dQ}/_{d\theta})_{app} + HA_{con}(T_{wall} - T)(^{dt}/_{d\theta})\right\}\left\{^{(\gamma-1)}/_{V}\right\} - \gamma(^{P}/_{V})\,(^{dV}/_{d\theta}) \quad (10)$$

The values of Convective heat loss rate, $HA_{con}(T_{wall} - T)(^{dt}/_{d\theta})$, Apparent rate of heat released, $(^{dQ}/_{d\theta})_{app}$, and Derivative of Volume, $(^{dV}/_{d\theta})$, are obtained from equations (3) - (9); and are put into equation (10).

The Euler's method was employed for the numerical integration of equation (3.10) starting with the initial conditions prevailing at the start of combustion (say at 340-degree crank angle during compression stroke with inlet and outlet valves closed). The final value of the pressure is then obtained by the reapplication of the Euler technique with the corrected slope. The above method was used by Sorenson for the Computer Simulation of Internal Combustion engine [12]. Numerical integration of equation (10) in conjunction with the equation of state, over the combustion period, gives the instantaneous temperature and pressure of the cylinder at some predetermined degree crank angle. The results were used in plotting the indicator diagram of the SI engine being simulated.

3.2 Simulation of intake process

Assuming a throttled engine, (i.e. $P_{exh} > P_{int.}$) In order to determine the instantaneous volume, Pressure, and temperature of the gas in the cylinder at any crank angle degree during the intake process, the following equations were used:

$$V_\theta = V_s/(CR - 1) + (\pi B^2/4)\left\{1 + r(1 - \cos\theta) - \sqrt{(l^2 - r^2\sin^2\theta)}\right\} \quad (8)$$

$$T_\theta = T_1(V_c/V_\theta)^{(\gamma 1-1)} \quad (11)$$

$$P_\theta = P_{44}(T_\theta/T_1)^{\gamma 1/(\gamma 1-1)} \quad (12)$$

Equations (11) and (12) above apply only to the isentropic expansion of the residual gas for a throttled engine when the inlet valve is at closed position. It was assumed that the inlet valve opens at a crank angle, θ_{int}, when the residual gas has expanded isentropically to the intake pressure $P_{int.}$

Thus, at any other crank angle ($\theta > \theta_{int}$) during the intake stroke, P_θ takes the value of P_{int}. Let the instantaneous volume, V_θ, and the instantaneous temperature, T_θ, at crank angle $\theta = \theta_{int}$ be denoted by V_{22} and $T_{22,}$ respectively.

Let V_{af} be the fuel-air intake at any degree crank angle during the intake process (at inlet valve open position) it follows that $V_{af} = V_\theta - V_{22}$.

Let the temperature of the mixture of fuel, air and the recycled exhaust gas be denoted by T_{intf} , and assuming the same specific heat capacity for the fuel-air mixture and the recycled exhaust gas, then it follows that T_{intf} and T_θ can be obtained using the following expressions:

$$T_{intf} = T_{44}(\%EGR)/100 + (1 - \%EGR/100)T_{int} \quad (13)$$

$$T_\theta = (T_{22}V_{22} + T_{intf}V_{af})/(V_{af} + V_{22}) \quad (14)$$

$$P_\theta = P_{int}$$

It is possible to get a more accurate estimate for the temperature of the intake charge if the specific heat capacities of the recycled exhaust gas and that of the air-fuel mixture are taken into consideration. However, for the purpose of this simulation, the intake temperature is fixed and does not vary with exhaust gas temperature at the end of the exhaust stroke. This assumption is reasonable if the recycled exhaust gas is cooled to the intake charge temperature before diluting the intake charge.

Equations (13) and (14) define the intake process from the time the intake valve opens to when it closes. The temperature at the end of the intake process, or at the beginning of the compression process is determined as follows:

$$T_2 = (1 - f)T_{int} + fT_{22} \quad (15)$$

The residual fraction, f, can be determined using the equation:

$$f = T_4P_{exh}/(T_{exh}P_4CR) \quad (16)$$

The mass of the in-cylinder gas just before compression begins is calculated using equation:

$$M_{afre} = P_{int}\, V_t\eta_v/(T_{int}R) \quad (17)$$

i.e. M_{afre} denotes mass of (air + fuel + residual gas + recycled exhaust gas) in the cylinder.

Mass of the unburned mixture in the cylinder just before compression begins is given by:

$$M_{af} = M_{afre} - M_e - M_r \quad (18)$$

or

$$M_{af} = M_{afe} - M_e \quad (19)$$

$$M_r = (M_{afre})f \quad (20)$$

or

$$M_r = P_{exh}V_c /(T_{exh}R) \quad (21)$$

$$M_{afe} = M_{afre} - M_r \quad (22)$$

$$M_e = (\%EGR(M_{afe}))/100 \quad (23)$$

3.3 Simulation of compression process

Equation (8) for calculating the instantaneous cylinder volume at any degree crank angle was used for the compression stroke.

$$T_\theta = T_2(V_t/V_\theta)^{(\gamma_1-1)} \quad (24)$$

$$P_\theta = P_{int}(T_\theta/T_2)^{\gamma_1/(\gamma_1-1)} \quad (25)$$

Equations (24) and (25) hold, assuming isentropic compression until combustion begins. As mentioned earlier in this section, equation (10) is integrated in order to determine the cylinder pressure and temperature during the combustion process.

3.4 Simulation of the expansion process

Let P_{33}, V_{33}, and T_{33} denote the pressure, volume, and temperature of the cylinder at the beginning of the expansion process, (e.g. at $\theta = 360^o$) respectively.

Equation (8) for calculating the instantaneous cylinder volume at any degree crank angle was also used for the expansion stroke.

$$T_\theta = T_{33}(V_{33}/V_\theta)^{(\gamma_2-1)} \quad (26)$$

$$P_\theta = P_{33}(T_\theta/T_{33})^{\gamma_2/(\gamma_2-1)} \quad (27)$$

Equations (26) and (27) hold for isentropic expansion until exhaust valves open.
P_4 = Pressure of the in-cylinder gas at the end of the expansion stroke.
T_4 = Temperature of the in-cylinder gas at the end of the expansion stroke.

3.5 Simulation of exhaust stroke

Equation (8) for calculating the Instantaneous cylinder Volume at any degree crank holds for the exhaust stroke.

$$P_\theta = P_{exh} \quad (28)$$

Equation (28) applies when the exhaust valve opens to allow all gases to flow out of the cylinder (i.e. the blowdown process).

Typically, the pressure ratio P_4/P_{exh} is such that sonic flow occurs at the valve so that blowdown is very quick and the constant volume approximation is justified [14] equation (28) is used during the constant pressure exhaustion stroke, and work is required to expel the gas.

The exhaust gas temperature at the end of the exhaust stroke is given by eqn. (29).

$$T_{exh} = T_4(P_{exh}/P_4)^{(\gamma_2-1)/\gamma_2} \quad (29)$$

$T_1 = T_{exh}$ (i.e. cylinder temperature at the beginning of the intake stroke).

$$V_{444} = V_t(P_4/P_{exh})^{1/\gamma_2} \quad (30)$$

$$f = V_c/V_{444} \quad (31)$$

3.6 Estimation of the quantity of recycled exhaust gas

A decision on the quantity of exhaust gas to be recycled is influenced by the peak cycle temperature of the previous cycle and the operation mode of the engine (whether decelerating or accelerating) In order to reduce NOx emission, a required amount of the recycled exhaust gas (EGR gas) is added to the intake charge so as to keep the peak cycle temperature to a minimum level.

Let %EGR be the percentage of the mass of the Recycled exhaust gas (M_e) to the mass of the Intake charge (M_{afe}).

That is,

%EGR= (Mass of recycled exhaust gas/mass of the intake gas) x 100% = (M_e/M_{afe}) x 100 (32)

But M_e can be expressed in terms of eqn. (23):

$$M_e = (\%EGR(M_{afe}))/100 \quad (23)$$

If the Intake process takes a period of θ_{int} crank angle, and for an engine speed of N rev/min; the mass flow rate of Recycled exhaust gas, M_{eN}, is estimated as a function of speed N, the mass of the intake charge, M_{afe}, and the mass of the fuel/air mixture, M_{af}.

Then for a four stroke engine,

$$M_{eN} = [(M_{afe} - M_{af})N(\theta_{int})]/86400 \quad (33)$$

If θ_{int} is assumed to be 180^o, i.e. the intake process takes a period of 180^o crank angle, then,

$$M_{eN} = [(M_{afe} - M_{af})N]/ 480 \quad (34)$$

Mass of fuel-air mixture, $\underline{M_{af}}$; mass of fuel-air mixture with recycled exhaust gas, M_{afe}; and the total mass of the in-cylinder gas, M_{afre}, are obtained from eqns.(17)-(22).

Equation (35) shows the relationship between M_{af}, M_{afe}, and %EGR.

$$M_{af} = M_{afe}(1 - \%EGR/100) \quad (35)$$

Let ΔT_{com} be the difference between peak combustion temperature T_{pk} and T_{all} (the permissible combustion temperature required for optimum or minimum exhaust pollutant emission). Then,

$$\Delta T_{com} = T_{pk} - T_{all} \tag{36}$$

It follows that when ΔT_{com} is positive; the EGR valve opens to recycle a calculated amount of exhaust gas to cool the combustion process to a lower temperature until the combustion temperature reaches T_{all}, and then the valve closes. When ΔT_{com} is negative, the EGR valve remains in a closed position as exhaust gas is not needed, so as not to hinder the smooth running of the engine.

%EGR estimation model:

$$\%EGR = f(\Delta T_{com}, T_{pk}, X_t) \tag{37}$$

X_t, which is the throttle position, is an indication of the load the engine is carrying, the engine speed, and air – fuel mass flow at a particular instant of time.

3.7 Simulation of EGR valve with considerations for its aerodynamic properties

Considering the 'pintle' valve section of an EGR system, as shown in Fig. 2. It is important to know the effect of the pintle valve on some thermodynamic properties of the EGR gas as well as the aerodynamic properties of the valve [15].

Let the initial conditions of the recycled exhaust gas at the entrance of the pintle valve be denoted by density,ρ_{e1}, pressure, P_{e1}, velocity, u_{e1}, velocity of sound, c_{e1}, Temperature, T_{e1}, and cross-sectional area perpendicular to flow, A_{e1}.

Let us assume isentropic conditions (i.e. frictionless flow.) This satisfactorily approximates the flow through short transitions, orifices, venturimeters and nozzles such that friction and heat transfer exhibit insignificant influences that may be ignored [16].

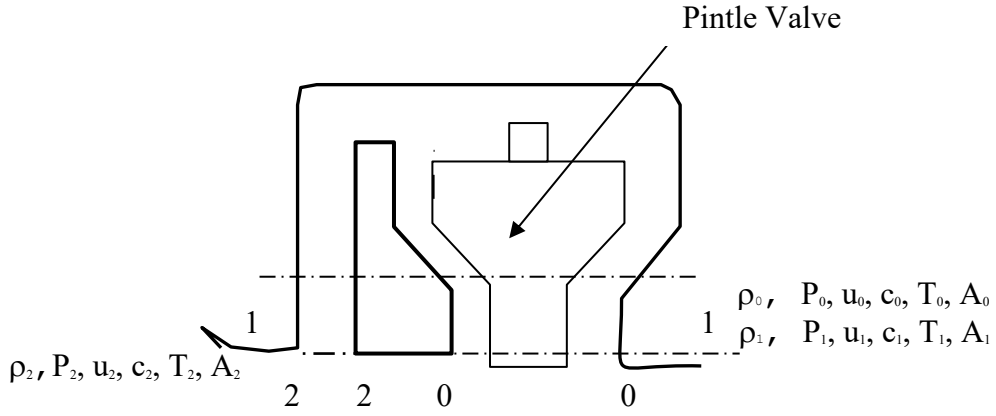

Fig. 2. EGR Valve

Applying the Euler energy equation for horizontal, frictionless flow:

$$(^{dP}/_{r}) + udu = 0 \tag{38}$$

But

$$^{dp}/_{d\rho} = c^2(^{d\rho}/_{r}) \tag{39}$$

Substituting eqn. (39) into eqn. (38) gives eqn. (40) i.e. Euler's equation for steady, frictionless flow.

$$c^2(^{d\rho}/_{r}) + udu = 0 \tag{40}$$

Applying the continuity equation to the EGR valve gives:

$$\rho\, u\, A = \text{constant} \tag{41}$$

Writing equation (41) in differential form gives:

$$(^{dr}/_{r}) + (^{du}/_{u}) + (^{dA}/_{A}) = 0 \tag{42}$$

Combining equations (40) and (42), we have:

$$(^{dA}/_{u}) = {}^{A}/_{u}\left\{ {}^{u^2}/_{c^2} - 1\right\} \tag{43}$$

Since $^{u}/_{c}$ = Ma, (Ma denotes Mach Number), then

$$(^{dA}/_{u}) = {}^{A}/_{u}\left\{ Ma^2 - 1\right\} \tag{44}$$

From the above equation (44), it is easy to explain the possible effect of the EGR valve on the recycled exhaust gas depending on the flow regime and the Mach number [17].

(i) If Ma < 1 (Subsonic flow), $(^{dA}/_{du})$ is always negative, meaning that, as the velocity increase, the cross-sectional area of the pintle valve must also increase.

(ii) If Ma = 1 (Sonic velocity), $(^{dA}/_{du}) = 0$; this is a case where the cross-sectional Area of the pintle valve must be a minimum for the flow velocity to equal that of sound.

(iii) If Ma > 1 (Supersonic flow), $(^{dA}/_{du})$ is always positive; here for the velocity to increase, the cross-sectional area of the pintle valve must also increase.

But our interest for the EGR valve is the subsonic or the sonic speed.

Hence, assuming 1-dimensional steady flow condition for the recycled exhaust gas flowing through the pintle valve into the intake manifold. Also, assume that the mechanical and thermodynamic characteristics of the recycled exhaust gas are uniform across the plane normal to the axis of the flow area of the pintle valve, then the equation for 1-dimensional steady compressible flow through an orifice or flow restriction can be applied to the EGR valve as follows.

The mass flow rate (kg/s) of the recycled exhaust gas, M_{eN}, is obtained from Equations (45)-(48).

For subsonic flow:

$$M_{eN} = \left[(C_d A_v P_{e1})/\sqrt{(RT_{e1})}\right]\left[{}^{2\gamma}/_{(\gamma-1)}\ \left\{(P_{e2}/P_{e1})^{2/\gamma} - (P_{e2}/P_{e1})^{(\gamma+1)/\gamma}\right\}\right]^{1/2} \tag{45}$$

$$(P_{e2}/P_{e1}) > [{}^{2}/_{(\gamma+1)}]^{\gamma/(\gamma+1)} \quad (46)$$

For sonic flow:

$$M_{eN} = [(C_d A_v P_{e1})/\sqrt{(RT_{e1})}]\,[\{{}^{2\gamma}/_{(\gamma+1)}\}^{(\gamma+1)/(\gamma-1)}]^{1/2} \quad (47)$$

$$(P_{e2}/P_{e1}) <= [{}^{2}/_{(\gamma+1)}]^{\gamma/(\gamma-1)} \text{ [18]} \quad (48)$$

Given the recycled gas mass flow rate, M_{eN} from eqn. (33) and putting the same into equation (45), then for a subsonic flow, the required area of the valve is determined by Equation (49) as follows:

$$A_v = [M_{eN}\sqrt{(RT_{e1})}]/\{C_d P_{e1}[{}^{2\gamma}/_{(\gamma-1)}((P_{e2}/P_{e1})^{2/\gamma} - (P_{e2}/P_{e1})^{(\gamma+1)/\gamma})]^{1/2}\} \quad (49)$$

Assuming adiabatic condition for the flow for which P/r^{γ} = constant, then the downstream temperature and velocity for maximum discharge is estimated as follows:

$$T_v = T_{e1}[{}^{2}/_{(\gamma+1)}] \quad (50)$$

$$U_v = (M_{eN}RT_v)/(C_d P_{e1}A_v) \quad (51)$$

However, EGR valve design should be for a case in which the pressure of the exhaust gas at the EGR valve outlet is just the same as that of the air-fuel mixture from the carburetor (approximately the atmospheric pressure) [19].

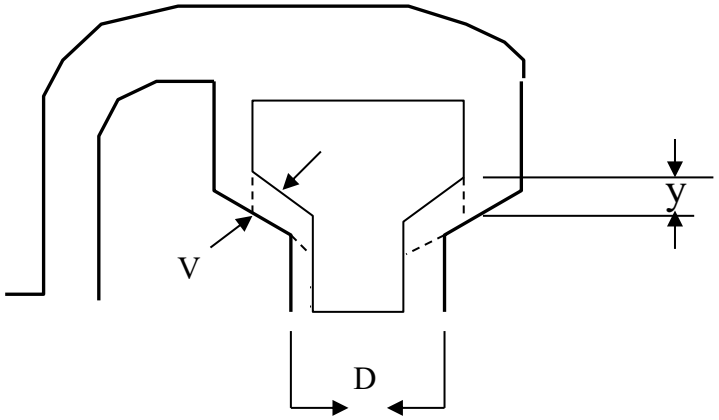

Fig. 3. The EGR pintle valve with the basic dimensions

Considering Figure 3, A_v is the cross-sectional area perpendicular to the direction of flow at the critical section "V"of the EGR valve.

The Area A_v is the surface area of an imaginary Frustum with diameter, D, and height, y. It is calculated as follows:

$$Av = \pi y(D - y\cot{}^{B}/_{2})\text{cosec}{}^{B}/_{2} \quad (52)$$

Where the height y is the 'vertical' distance (or lift) that the pintle valve must be moved in order to introduce a calculated quantity of recycled exhaust gas into the intake manifold. The Area, A_v, of the EGR valve can be calculated from equations (45)-(48).

Once the area, A_v, of the EGR has been determined, the valve lift, y, can then be estimated using equation (52).

$$y = [\pi D \pm \sqrt{(\pi^2 D^2 - 4\pi A_v \cos^B/_2)}]/(2\pi \cot^B/_2) \quad (53)$$

where D and B are the basic EGR valve dimensions as shown in Figure 3, and the area Av, is the slanting surface area of an imaginary Frustum with base diameter D, and perpendicular height, y.

A_v varies with the "vertical" lift, y, of the valve.
When y = 0, A_V = 0, (i.e. Valve at closed position).
When y = maximum, A_V = maximum, (i.e. valve at fully open position).

3.8 Simulation of indicated work, power and thermal efficiency

The Indicated Power, IP, is defined as the actual rate of work done by the working fluid on the piston. IP can be determined from the indicated diagram. The Actual work done by the engine can be estimated from the integral of force on the piston with respect to the distance moved by the piston, or integral of pressure in the cylinder with respect to volume, provided that the variation of average pressure in the cylinder is plotted during the machine cycle [20]. The indicated mean effective pressure, P_{imep}, is defined as the height of a rectangle on the P-V diagram having the same length and area as the cycle. This implies that the work done, W, can be estimated using the indicated mean effective pressure P_{imep}.

$$W = \text{Integral of } (PdV) = P_{imep}V_s \quad (54)$$

Hence, the Indicated Power, I.P. can be estimated as follows:
$I.P. = 100P_{imep}SA_pN'$
where S is the stroke in m,
A_p is the piston head area in m^2,
P_{imep} is the indicated mean effective pressure in bar,
N' is the number of revolutions per second (it is $N/_2$ rev/s for a four-stroke engine and Nrev/s for a two-stroke engine.

The indicated mean effective pressure can also be estimated using equation (55) as follows [14]:

$$P_{imep} = (M_f(LHV)\eta_i CR)/(V_2(CR-1)) \quad (55)$$

Indicated Thermal efficiency was calculated using eqn. (56):

$$\eta_i = W_i/(M_f(LHV)) \quad (56)$$

where W_i and M_f denote indicated work in KJ, and Mass of fuel consumed per cycle in Kg respectively.

4. SOLUTION METHODOLOGY

The method employed in the simulation of factors affecting the EGR system as a means of emission control is an iterative process whereby cycle temperature is modeled and controlled by the dilution of the intake air-fuel mixture with some pre-determined quantities of recycled exhaust gas.

The basic input variables needed for the determination of the cycle temperature include: engine bore, piston stroke, connecting rod length, engine speed (revolutions/minute), combustion duration, fuel heating value, cylinder wall temperature, intake pressure, exhaust pressure, throttle position, specific heat ratios and ambient temperature.

Thermodynamics models were used for the simulation/estimation of the cycle temperature and pressure of an SI engine. Some basic engine data for a spark ignition CFR engine were used. A preset maximum allowable temperature that gives minimum emission and optimum engine performance was assumed (say 2000K). A sub-model gets a given%EGR and determines the peak cycle temperature and pressure. Other engine parameters are also determined for each cycle at a given%EGR. The graphs of the cycle temperature and pressure, and other performance parameters such as P_{imep}, residual fraction, indicated thermal efficiency, are therefore plotted against%EGR. Relationships obtained from the graphs, such as equations or trends showing the variation of various engine performance parameters with the%EGR can be used in mapping out the optimum quantity of exhaust gas needed to dilute the intake charge. Such relations are equally useful for the design of the EGR valve control system. Upon the introduction of a predetermined quantity of exhaust gas into the intake manifold, the fresh intake is further diluted, and subsequent reduction of peak cycle temperature is achieved [21]. Figure 4 shows the simulation model flow chart for the method used.

Expected output from the models:

1. Mass flow rate of exhaust gas through the EGR valve (M_e).
2. Velocity of exhaust gas at the point of recirculation (u_e).
3. Temperature of exhaust gas at the point of recirculation (T_e).
4. EGR Pintle valve lift (y).
5. Peak Cycle Temperature (or combustion peak temperature) (T_{pk}).
6. Peak Cycle Pressure (or combustion peak pressure) (P_{pk}).
7. Throttle position (X_t).
8. Engine speed (N).
9. Indicated Thermal efficiency (η_i).
10. Volumetric efficiency (η_V).

4.1 Programming

An iterative BASIC program was developed to use the various models / equations listed earlier, to determine the pressure, and temperature of the cylinder at any crank angle degree. The program was developed to calculate the indicated effective mean pressure, work, power, efficiency, residual fraction, EGR valve lift, and EGR velocity. The BASIC program was written in modules and subroutines to handle various sub-models. The Compiler used was QuickBasic Version 4.5, for the Microsoft Disk Operating System. The Output from running the program was written by the computer directly into three output files where the results were accessed and used to plot graphs on Microsoft Excel. The Basic program used is excluded from the work for compactness of the report.

The simulation model flow diagram for the sub-models is shown in Figure 5.

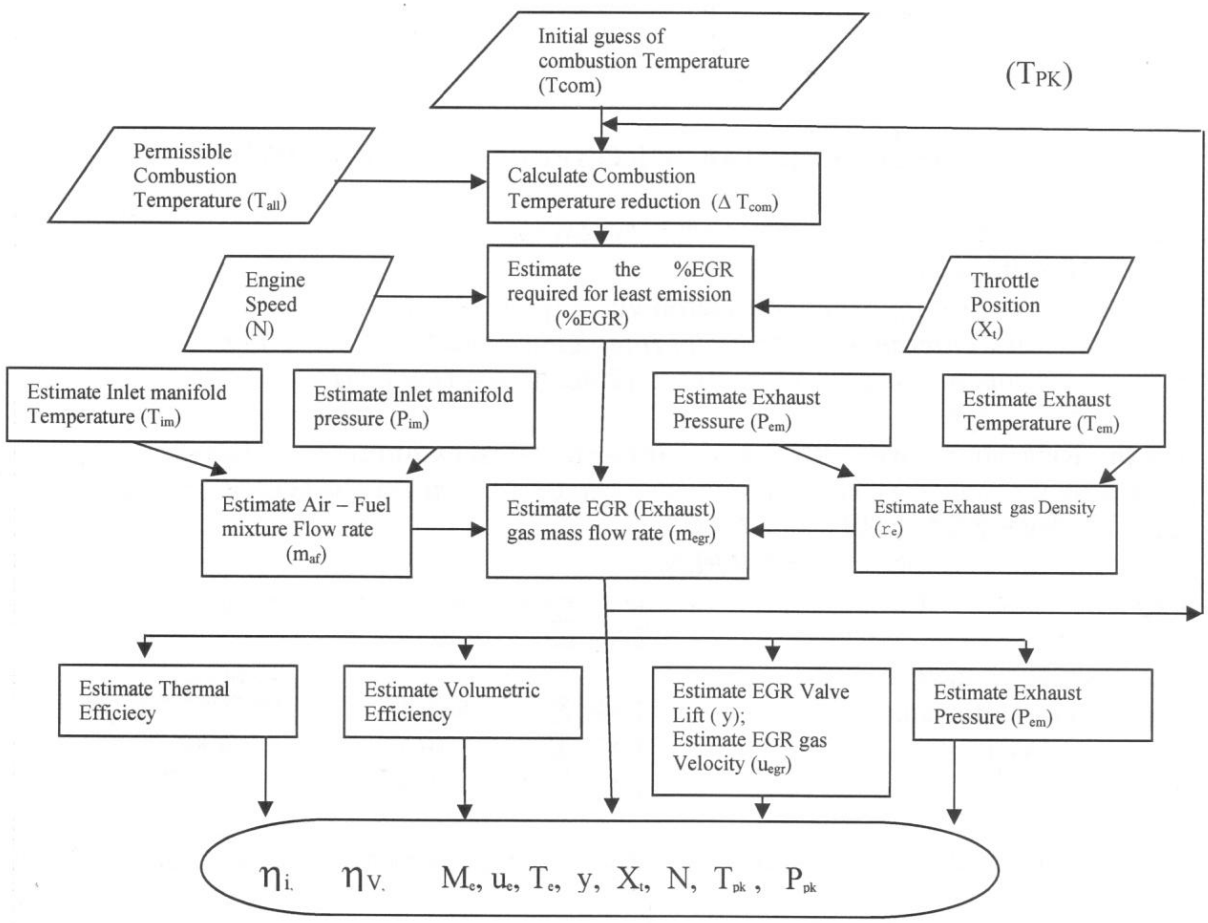

Fig. 4. Overall model flow chart for the simulation of basic factors affecting EGR system as a means of emission control

5. RESULTS AND DISCUSSION

Table 1 shows the engine parameters used in the simulation process for the purpose of ensuring the accuracy, validity and replicability of the suggested computational approach in this study.

Tab. 1

Engine parameters used for the SI engine simulation

Engine Type: CFR Engine	
Parameter:	Value:
Bore	82.6mm
Stroke	114.3mm
Connecting rod length	338.7mm
Speed	1800rev/min
Combustion duration	40° (crank angle)
Fuel heating value	44000 kJ/kg
Cylinder wall Temperature	450°K
Intake Pressure	95 kPa

Intake Temperature	330 ^{o}K
Exhaust Pressure	105 kPa
Fuel-Air Ratio	0.065
Compression Ratio	7
Start of Combustion	340^{o} (crank angle)

The Outputs from the Basic program are shown in Tables 2 to 6. Table 2 shows the volume and pressure at any degree crank angle, for a complete cycle at 0%EGR. Table 2 reflects the baseline combustion characteristics for the SI engine investigated in a situation that the engine runs but without exhaust gases present, to be recycled back into the cylinder. The simulated data is fundamental in engine research to compare performance, combustion and emission results for optimization purposes.

Tab. 2

Simulated data on Instantaneous Volume, Pressure, and Temperature of an SI engine at 0%, EGR

Crank angle (Degree)	Temperature (K)	Volume m^3	Pressure kPa	Crank angle (Degree)	Temperature (K)	Volume m^3	Pressure kPa
0	1295.034	1.02E-04	105	360	2876.973	1.02E-04	5681.485
10	1260.884	1.11E-04	95	370	2817.734	1.11E-04	5120.154
20	1087.007	1.36E-04	95	380	2674.907	1.37E-04	3947.537
30	911.6299	1.77E-04	95	390	2504.116	1.78E-04	2838.28
40	774.3091	2.32E-04	95	400	2341.156	2.33E-04	2027.379
50	675.9077	2.98E-04	95	410	2199.322	2.99E-04	1483.292
60	606.8663	3.72E-04	95	420	2080.473	3.73E-04	1123.552
70	558.1528	4.52E-04	95	430	1982.422	4.53E-04	882.598
80	523.2751	5.33E-04	95	440	1902.064	5.35E-04	717.6434
90	497.8994	6.14E-04	95	450	1836.457	6.15E-04	602.1256
100	479.1747	6.91E-04	95	460	1783.1	6.92E-04	519.5906
110	465.2137	7.62E-04	95	470	1739.95	7.63E-04	459.6911
120	454.7498	8.26E-04	95	480	1705.366	8.27E-04	415.787
130	446.9209	8.82E-04	95	490	1678.047	8.82E-04	383.5332
140	441.1349	9.28E-04	95	500	1656.969	9.28E-04	360.0438
150	436.9848	9.64E-04	95	510	1641.351	9.64E-04	343.3919
160	434.1956	9.89E-04	95	520	1630.613	9.90E-04	332.3054
170	432.5906	1.00E-03	95	530	1624.359	1.00E-03	325.982
180	432.0712	1.01E-03	95	540	1622.36	1.01E-03	323.9808
190	294.9453	1.00E-03	60.41652	550	1295.034	1.00E-03	105
200	296.4752	9.89E-04	61.6895	560	1295.034	9.89E-04	105
210	299.087	9.63E-04	63.90926	570	1295.034	9.63E-04	105
220	302.8846	9.27E-04	67.24313	580	1295.034	9.26E-04	105
230	308.0198	8.81E-04	71.95737	590	1295.034	8.80E-04	105
240	314.7011	8.25E-04	78.45779	600	1295.034	8.25E-04	105
250	323.2039	7.61E-04	87.35748	610	1295.034	7.60E-04	105
260	333.8859	6.90E-04	99.58968	620	1295.034	6.89E-04	105
270	347.2074	6.13E-04	116.5985	630	1295.034	6.12E-04	105
280	363.7562	5.32E-04	140.6666	640	1295.034	5.31E-04	105
290	384.2747	4.51E-04	175.4845	650	1295.034	4.49E-04	105
300	409.6716	3.71E-04	227.121	660	1295.034	3.70E-04	105

310	440.965	2.97E-04	305.5618	670	1295.034	2.96E-04	105
320	478.9999	2.31E-04	426.4941	680	1295.034	2.30E-04	105
330	523.5444	1.77E-04	610.3176	690	1295.034	1.76E-04	105
340	571.0413	1.36E-04	866.0734	700	1295.034	1.35E-04	105
350	1984.9	1.10E-04	3623.022	710	1295.034	1.10E-04	105
				720	1295.034	1.02E-04	105

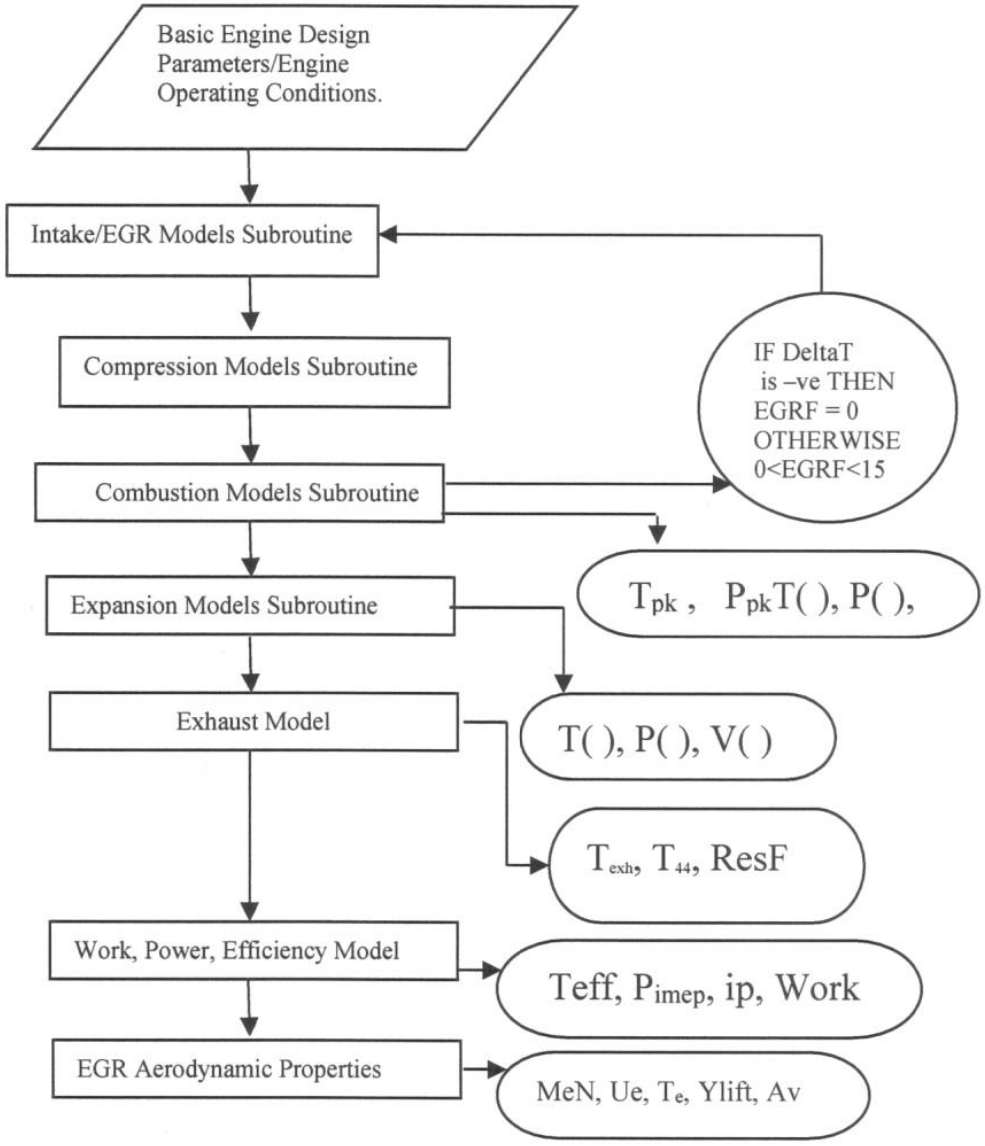

Fig. 5. Flow chart showing basic program main modules and sub-routines for the simulation of the effects of exhaust gas recirculation emission control system on SI engine performance parameters

Table 3 shows the volume and pressure at any degree crank angle, for the complete cycles at 0%, 5%, 10%, 15% and 20% EGR. Table 3 is essential, helping the researcher to coduct a comprehensive thermodynamic analysis and combustion trend monitoring for the S.I. engine investigated. Furthermore, Table 3 data serves as a critical disgnostic tool that may assist also to gain insight of the combustion behaviour, emission formation mechanism and performance of the engine.

Table 4 shows the volume and temperature at any degree crank angle, for complete cycle at 0%, 5%, 10%, 15%, and 20% EGR. Table 4 reveals the characteristics of the in-cylinder thermodynamic process and provides insights on the emission reductions while attempting to optimize engine performance. Moreover, Table 4 is useful to gain insight into how emissions, thermodynamic performance and combustion attributed of the engine are influenced by the EGR.

Tab. 3

Simulated data on instantaneous volume, pressure of an SI engine, at 0%, 5%, 10%, 15%, and 20% EGR

Crank angle	Volume m^3	Pressure at 0%EGR (kPa)	Pressure at 5%EGR (kPa)	Pressure at 10%EGR (kPa)	Pressure at 15%EGR (kPa)	Pressure at 20%EGR (kPa)
0	1.02E-04	105	105	105	105	105
20	1.36E-04	95	95	95	95	95
40	2.32E-04	95	95	95	95	95
60	3.72E-04	95	95	95	95	95
80	5.33E-04	95	95	95	95	95
100	6.91E-04	95	95	95	95	95
120	8.26E-04	95	95	95	95	95
140	9.28E-04	95	95	95	95	95
160	9.89E-04	95	95	95	95	95
180	1.01E-03	95	95	95	95	95
200	9.89E-04	61.6895	61.6895	61.6895	61.6895	61.6895
220	9.27E-04	67.24313	67.24313	67.24313	67.24313	67.24313
240	8.25E-04	78.45779	78.45779	78.45779	78.45779	78.45779
260	6.90E-04	99.58968	99.58968	99.58968	99.58968	99.58968
280	5.32E-04	140.6666	140.6666	140.6666	140.6666	140.6666
300	3.71E-04	227.121	227.121	227.121	227.121	227.121
320	2.31E-04	426.4941	426.4941	426.4941	426.4941	426.4941
340	1.36E-04	866.0734	866.0734	866.0734	866.0734	866.0734
350	1.10E-04	3623.022	3567.263	3513.04	3460.312	3409.035
360	1.02E-04	5681.485	5562.251	5446.967	5335.511	5227.763
380	1.37E-04	3947.537	3864.694	3784.593	3707.151	3632.288
400	2.33E-04	2027.379	1984.832	1943.694	1903.922	1865.474
420	3.73E-04	1123.552	1099.973	1077.175	1055.134	1033.826
440	5.35E-04	717.6434	702.5826	688.0208	673.9424	660.3325
460	6.92E-04	519.5906	508.6863	498.1431	487.9501	478.0962
480	8.27E-04	415.787	407.0612	398.6244	390.4677	382.5824
500	9.28E-04	360.0438	352.4878	345.1821	338.1189	331.2908
520	9.90E-04	332.3054	325.3315	318.5886	312.0696	305.7676
540	1.01E-03	323.9808	317.1816	310.6077	304.252	298.1078
560	9.89E-04	105	105	105	105	105
580	9.26E-04	105	105	105	105	105
600	8.25E-04	105	105	105	105	105
620	6.89E-04	105	105	105	105	105
640	5.31E-04	105	105	105	105	105
660	3.70E-04	105	105	105	105	105
680	2.30E-04	105	105	105	105	105
700	1.35E-04	105	105	105	105	105
720	1.02E-04	105	105	105	105	105

Tab. 4

Simulated data on Instantaneous Volume and Temperature of an SI engine, at 0%, 5%, 10%, 15%, and 20%EGR

Crank angle (degree)	Volume m^3	Temperature at 0%EGR (K)	Temperature at 5%EGR (K)	Temperature at 10%EGR (K)	Temperature at 15%EGR (K)	Temperature at 20%EGR (K)
0	1.02E-04	1295.034	1273.246	1252.09	1231.552	1211.615
20	1.36E-04	1087.007	1080.222	1073.268	1066.172	1058.96
40	2.32E-04	774.3091	793.473	811.0558	827.1611	841.8865
60	3.72E-04	606.8663	639.9252	670.6469	699.1759	725.6486
80	5.33E-04	523.2751	563.2708	600.5517	635.2828	667.6201
100	6.91E-04	479.1747	522.83	563.5714	601.5746	637.0057
120	8.26E-04	454.7498	500.432	543.0899	582.9054	620.0502
140	9.28E-04	441.1349	487.9468	531.6732	572.4988	610.5988
160	9.89E-04	434.1956	481.5834	525.8542	567.1948	605.7815
180	1.01E-03	432.0712	479.6353	524.0728	565.5709	604.3068
200	9.89E-04	296.4752	296.4752	296.4752	296.4752	296.4752
220	9.27E-04	302.8846	302.8846	302.8846	302.8846	302.8846
240	8.25E-04	314.7011	314.7011	314.7011	314.7011	314.7011
260	6.90E-04	333.8859	333.8859	333.8859	333.8859	333.8859
280	5.32E-04	363.7562	363.7562	363.7562	363.7562	363.7562
300	3.71E-04	409.6716	409.6716	409.6716	409.6716	409.6716
320	2.31E-04	478.9999	478.9999	478.9999	478.9999	478.9999
340	1.36E-04	571.0413	571.0413	571.0413	571.0413	571.0413
350	1.10E-04	2876.973	2816.596	2758.219	2701.78	2647.219
360	1.02E-04	2674.907	2618.771	2564.493	2512.019	2461.29
380	1.37E-04	2341.156	2292.024	2244.519	2198.592	2154.192
400	2.33E-04	2080.473	2036.812	1994.596	1953.783	1914.327
420	3.73E-04	1902.064	1862.147	1823.552	1786.238	1750.166
440	5.35E-04	1783.1	1745.679	1709.498	1674.518	1640.702
460	6.92E-04	1705.366	1669.577	1634.973	1601.518	1569.176
480	8.27E-04	1656.969	1622.196	1588.574	1556.068	1524.644
500	9.28E-04	1630.613	1596.392	1563.305	1531.317	1500.393
520	9.90E-04	1622.36	1588.313	1555.393	1523.567	1492.799
540	1.01E-03	1295.034	1273.246	1252.09	1231.552	1211.615
560	9.89E-04	1295.034	1273.246	1252.09	1231.552	1211.615
580	9.26E-04	1295.034	1273.246	1252.09	1231.552	1211.615
600	8.25E-04	1295.034	1273.246	1252.09	1231.552	1211.615
620	6.89E-04	1295.034	1273.246	1252.09	1231.552	1211.615
640	5.31E-04	1295.034	1273.246	1252.09	1231.552	1211.615
660	3.70E-04	1295.034	1273.246	1252.09	1231.552	1211.615
680	2.30E-04	1295.034	1273.246	1252.09	1231.552	1211.615
700	1.35E-04	1295.034	1273.246	1252.09	1231.552	1211.615
720	1.02E-04	1295.034	1273.246	1252.09	1231.552	1211.615

Tables 5 and 6 show the indicated work, thermal efficiency, indicated power, specific heat ratio, EGR valve lift, EGR gas flow rate, air-fuel flow rate, cylinder peak temperature, residual fraction, Work per unit mass of fuel, cylinder peak pressure, and EGR gas downstream velocity, at 0-30% EGR. Tables 5 and 6 were created for the purposes of assessing, optimizing and balacing the nitrogen oxide emission reduction-performance tradeoff.

Tab. 5

Simulated data on Indicated Work, Thermal efficiency, Power, Air-Fuel flow rate, Cylinder Peak Temperature and Pressure, Residual fraction, Work per unit mass of fuel, EGR gas downstream velocity, at 0%, 5%, 10%, 15%, and 20%EGR

%EGR: (%)	Work (kJ)	Volumetric efficiency	Thermal efficiency: (%)	Indicated power: (kW)	Specific heat ratio	Y lift (mm)	EGR mass flow rate (kg/s)
0	0.393004	0.98	20.73407	5.895064	1.25	0	0
1	0.390854	0.98	20.83198	5.862816	1.247225	0.142063	2.62E-05
2	0.388719	0.98	20.93266	5.83079	1.244457	0.288362	5.23E-05
3	0.386598	0.98	21.03613	5.798969	1.241694	0.439303	7.85E-05
4	0.384491	0.98	21.14254	5.76737	1.238938	0.595363	1.05E-04
5	0.382399	0.98	21.25196	5.735986	1.236188	0.757107	1.31E-04
6	0.380321	0.98	21.36443	5.704807	1.233444	0.92521	1.57E-04
7	0.378256	0.98	21.48009	5.673837	1.230706	1.100494	1.83E-04
8	0.376205	0.98	21.59904	5.64308	1.227974	1.283975	2.09E-04
9	0.374168	0.98	21.72136	5.612525	1.225248	1.476932	2.35E-04
10	0.372145	0.98	21.84717	5.582176	1.222529	1.681015	2.61E-04
11	0.370136	0.98	21.9766	5.552034	1.219815	1.898418	2.87E-04
12	0.36814	0.98	22.10975	5.522094	1.217107	2.132164	3.13E-04
13	0.366157	0.98	22.24675	5.492361	1.214406	2.386631	3.40E-04
14	0.364188	0.98	22.3877	5.462819	1.21171	2.668583	3.66E-04
15	0.362232	0.98	22.53277	5.433477	1.20902	2.989534	3.92E-04
16	0.360289	0.98	22.68209	5.404337	1.206336	3.372348	4.18E-04
17	0.35836	0.98	22.83584	5.375397	1.203659	3.878516	4.44E-04
18	0.356443	0.98	22.99409	5.346642	1.200987	4.643327	4.70E-04
19	0.354539	0.98	23.15709	5.318087	1.198321		4.96E-04
20	0.352649	0.98	23.32499	5.289727	1.195661		5.22E-04
21	0.35077	0.98	23.49794	5.261554	1.193007		5.48E-04
22	0.348905	0.98	23.67616	5.233574	1.190359		5.74E-04
23	0.347052	0.98	23.85984	5.205783	1.187716		6.00E-04
24	0.345212	0.98	24.0492	5.178182	1.18508		6.26E-04
25	0.343385	0.98	24.24445	5.150767	1.182449		6.52E-04
26	0.341569	0.98	24.44583	5.123537	1.179825		6.78E-04
27	0.339766	0.98	24.65357	5.096488	1.177206		7.04E-04
28	0.337975	0.98	24.86796	5.06963	1.174593		7.30E-04
29	0.336196	0.98	25.08923	5.042946	1.171985		7.56E-04
30	0.33443	0.98	25.31771	5.016446	1.169384		7.81E-04

Tab. 6

Simulated data on Indicated Work, Thermal efficiency, Power, Air-Fuel flow rate, Cylinder Peak Temperature and Pressure, Residual fraction, Work per unit mass of fuel, EGR gas downstream velocity, at 0%, 5%, 10%, 15%, and 20%EGR

%EGR: (%)	Air/fuel flow rate (kg/s)	Peak cycle temperature (K)	Peak cycle pressure (kPa)	Residual fraction	IMEP (kPa)	Work/Mass (kJ/kg)	EGR gas velocity (m/s)
0	2.47E-03	2876.973	5681.485	5.80E-02	641.3962	9122.991	0
1	2.45E-03	2864.735	5657.317	5.82E-02	637.8875	9166.073	3.802116
2	2.42E-03	2852.579	5633.311	0.058398	634.403	9210.372	3.802116
3	2.40E-03	2840.503	5609.462	5.86E-02	630.9408	9255.899	3.802116
4	2.37E-03	2828.508	5585.776	5.88E-02	627.5027	9302.717	3.802116
5	2.35E-03	2816.596	5562.251	5.90E-02	624.0881	9350.86	3.802116
6	2.32E-03	2804.762	5538.882	5.92E-02	620.6957	9400.351	3.802116
7	2.30E-03	2793.009	5515.67	5.94E-02	617.3262	9451.239	3.802116
8	2.27E-03	2781.334	5492.616	5.96E-02	613.9797	9503.579	3.802116
9	2.25E-03	2769.738	5469.715	5.98E-02	610.6552	9557.399	3.802116
10	2.22E-03	2758.219	5446.967	6.00E-02	607.3532	9612.756	3.802116
11	2.20E-03	2746.778	5424.374	6.02E-02	604.0737	9669.704	3.802116
12	2.17E-03	2735.414	5401.932	6.04E-02	600.8162	9728.288	3.802116
13	2.15E-03	2724.128	5379.644	6.06E-02	597.5811	9788.572	3.802116
14	2.12E-03	2712.916	5357.502	6.08E-02	594.3669	9850.589	3.802116
15	2.10E-03	2701.78	5335.511	6.10E-02	591.1745	9914.417	3.802116
16	2.07E-03	2690.719	5313.668	6.12E-02	588.0039	9980.12	3.802116
17	2.05E-03	2679.734	5291.974	6.14E-02	584.8552	10047.77	3.802116
18	2.02E-03	2668.822	5270.424	6.16E-02	581.7266	10117.4	3.802116
19	2.00E-03	2657.983	5249.02	6.18E-02	578.6198	10189.12	3.802116
20	1.97E-03	2647.219	5227.763	6.20E-02	575.5341	10262.99	3.802116
21	1.95E-03	2636.526	5206.647	6.22E-02	572.4689	10339.09	3.802116
22	1.92E-03	2625.906	5185.674	6.24E-02	569.4246	10417.51	3.802116
23	1.90E-03	2615.357	5164.843	6.26E-02	566.4008	10498.33	3.802116
24	1.87E-03	2604.881	5144.154	6.28E-02	563.3978	10581.65	3.802116
25	1.85E-03	2594.475	5123.604	6.30E-02	560.4149	10667.56	3.802116
26	1.82E-03	2584.14	5103.193	6.32E-02	557.4523	10756.17	3.802116
27	1.80E-03	2573.873	5082.919	6.34E-02	554.5093	10847.57	3.802116
28	1.77E-03	2563.678	5062.786	6.36E-02	551.5871	10941.9	3.802116
29	1.75E-03	2553.551	5042.787	0.063807	548.6838	11039.26	3.802116
30	1.72E-03	2543.493	5022.924	6.40E-02	545.8005	11139.79	3.802116

Table 7 shows data on crank angle ratio, mass burnt fraction, instantaneous heat release rate and heat release ratio at crank angles mapped to the combustion duration.

Tab. 6

Simulated data on crank angle ratio, mass burnt fraction, instantaneous heat release rate and heat release ratio at crank angles corresponding to the combustion duration

Crank angle (degree)	Crank angle ratio	Heat released rate (kJ/degree)	Heat released ratio
340	0	0	0
342	0.05	3.71E-03	0.156497
344	0.1	7.32E-03	0.309137
346	0.15	1.08E-02	0.45416
348	0.2	1.39E-02	0.58799
350	0.25	1.68E-02	0.70733
352	0.3	1.92E-02	0.80924
354	0.35	0.021116	0.891208
356	0.4	2.25E-02	0.951213
358	0.45	2.34E-02	0.987777
360	0.5	2.37E-02	1
362	0.55	2.34E-02	0.98758
364	0.6	2.25E-02	0.950822
366	0.65	0.021102	0.890633
368	0.7	1.92E-02	0.808497
370	0.75	1.67E-02	0.706436
372	0.8	1.39E-02	0.586967
374	0.85	1.07E-02	0.453033
376	0.9	7.30E-03	0.307935
378	0.95	3.68E-03	0.155248
380	1	-3.00E-05	-1.26E-03

Note the following description of the four-stroke cycle simulated:
Crank angle 0º is taken as Top Dead Centre (TDC)
Crank angle 180º is taken as Bottom Dead Centre (BDC)
Crank angle 360º is taken as TDC
Crank angle 540º is taken as BDC
Crank angle 720º is taken as TDC

Intake Stroke: 0º - 180º crank angle
Compression Stroke: 180º - 360º crank angle
Expansion Stroke: 360º - 540º crank angle
Exhaust Stroke 540º - 720º crank angle
Combustion duration: 340º - 380º crank angle

Figures 6 to 25 show the graphs generated from the results of the simulation. The results are discussed as follow with emphasis on how the various engine performance parameters vary with %EGR. Figure 6 shows the simulated P-V indicator diagram for an S.I. engine at %EGR. Figure 7 presents the simulated pressure vs. Crank angle indicator diagram for an S.I. engine at %EGR = 0%. In Figure 8, the simulated temperature vs. crank angle indicator diagram for

an S.I. engine at %EGR = 0% is indicated. Figure 9 shows the simulated indicator PV diagram for an S.I. engine for varying percentage recycled exhaust gas (%EGR). In Figure 10, the simulated indicated pressure vs. Degree crank angle of an S.I. engine at 0%, 5%, 10%, 15% and 20% recycled exhaust gas (%EGR) is presented. Figure 11 shows the indicated temperatures vs. Degree crank angles of an S.I. engine at 0%, 5%, 10%, 15% and 20% recycled exhaust gas (%EGR).

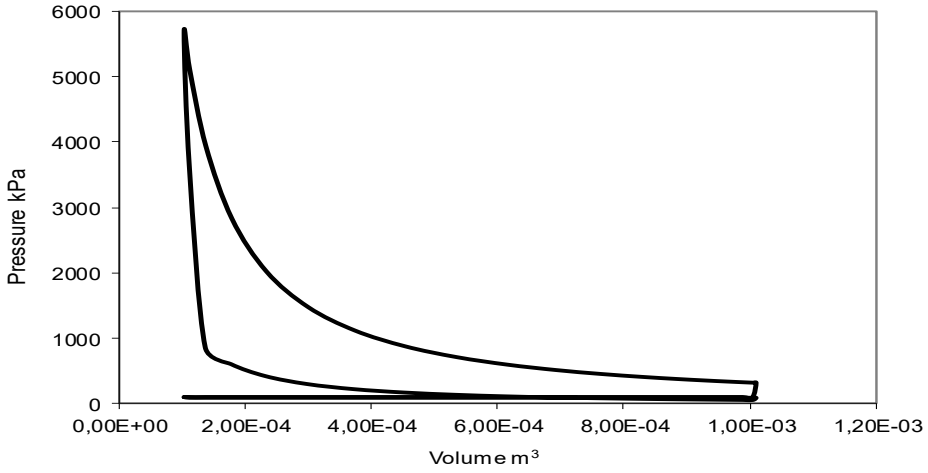

Fig. 6. Simulated P-V indicator diagram for an S.I. engine at %EGR

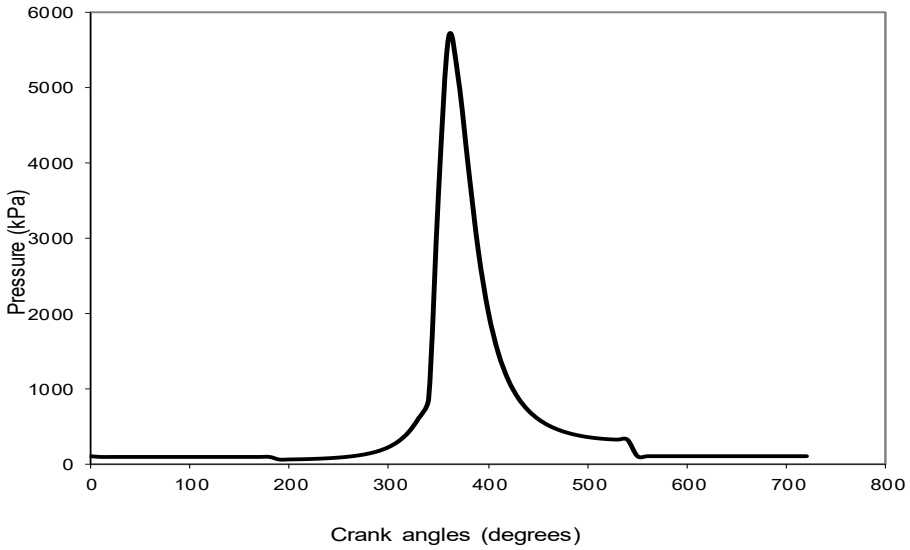

Fig. 7. Simulated pressure vs. Crank angle indicator diagram for an S.I. engine at %EGR = 0%

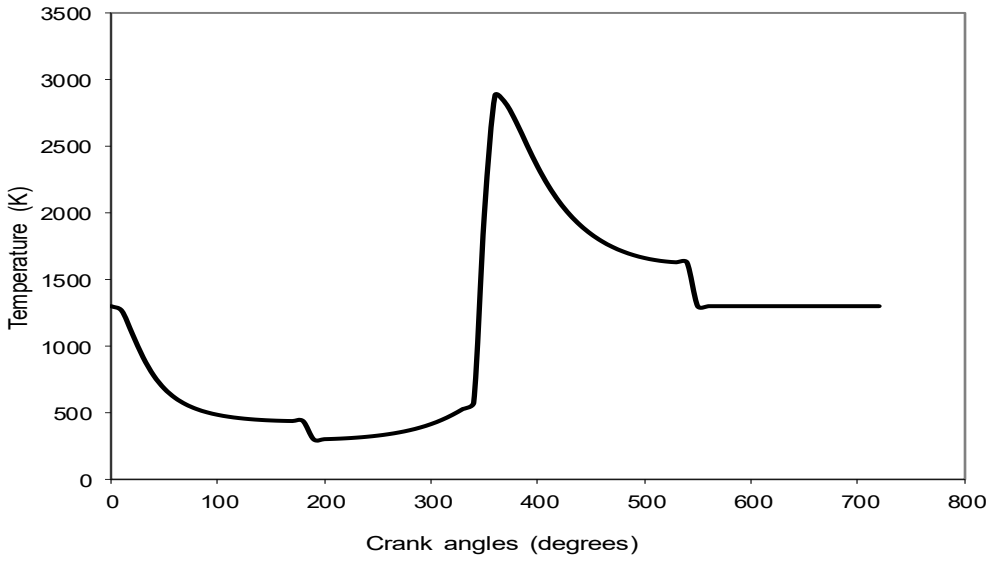

Fig. 8. Simulated temperature vs. Crank angle indicator diagram for an S.I. engine at %EGR = 0%

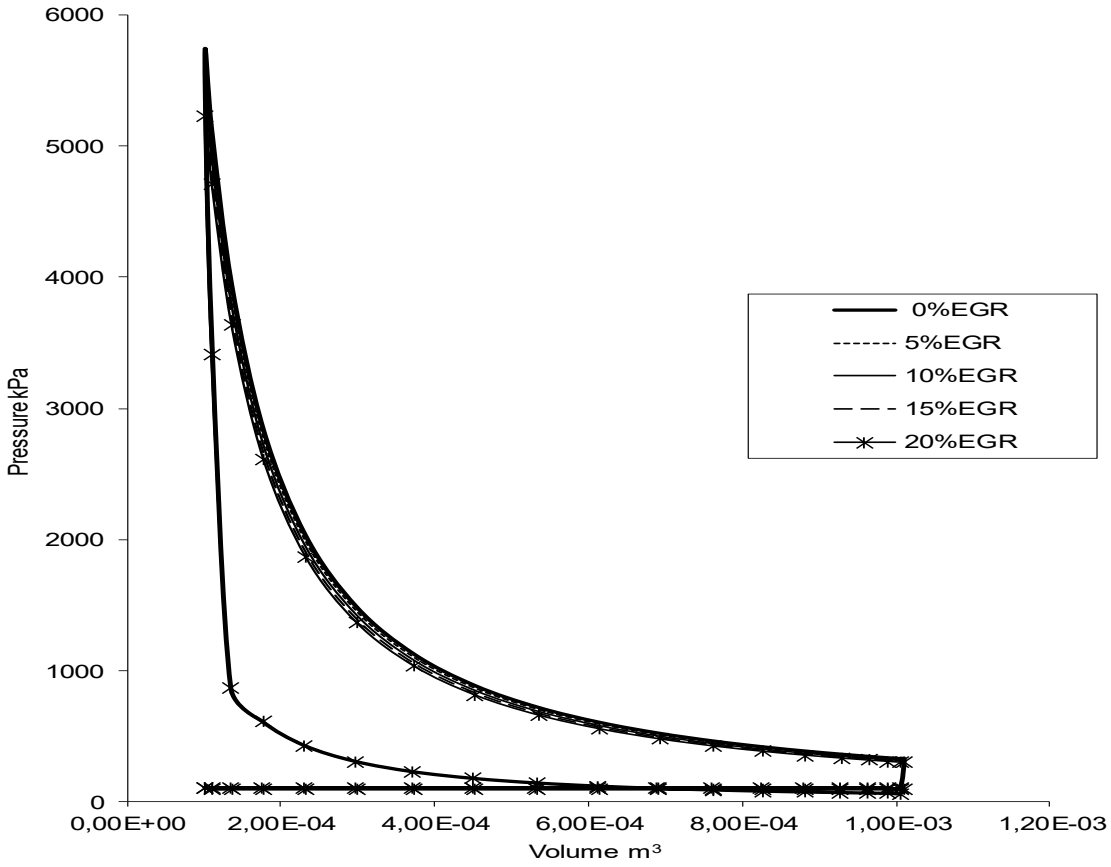

Fig. 9. Simulated indicator PV diagram for an S.I. engine for varying percentage recycled exhaust gas (%EGR)

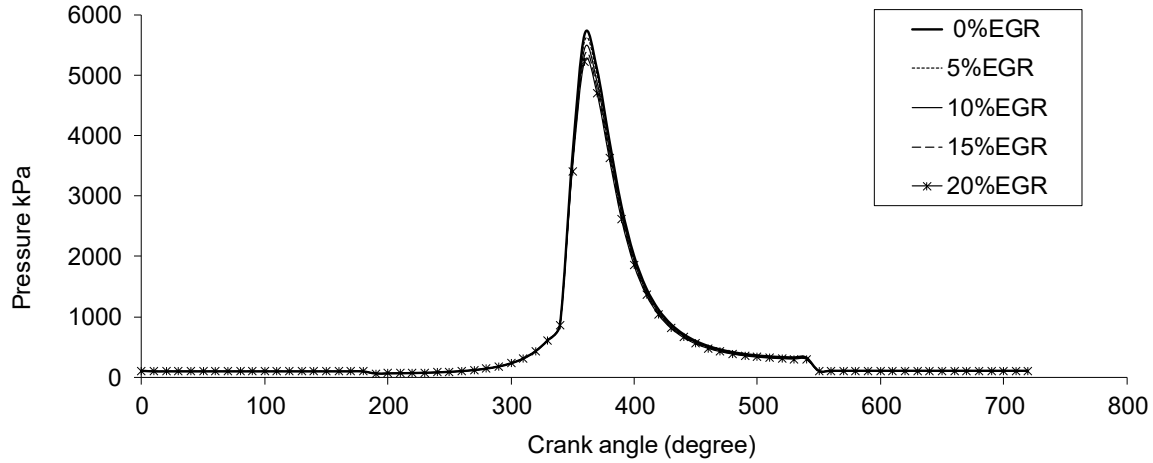

Fig. 10. Simulated indicated pressure Vs. Degree crank angle of an S.I. engine at 0%, 5%, 10%, 15% and 20% recycled exhaust gas (%EGR)

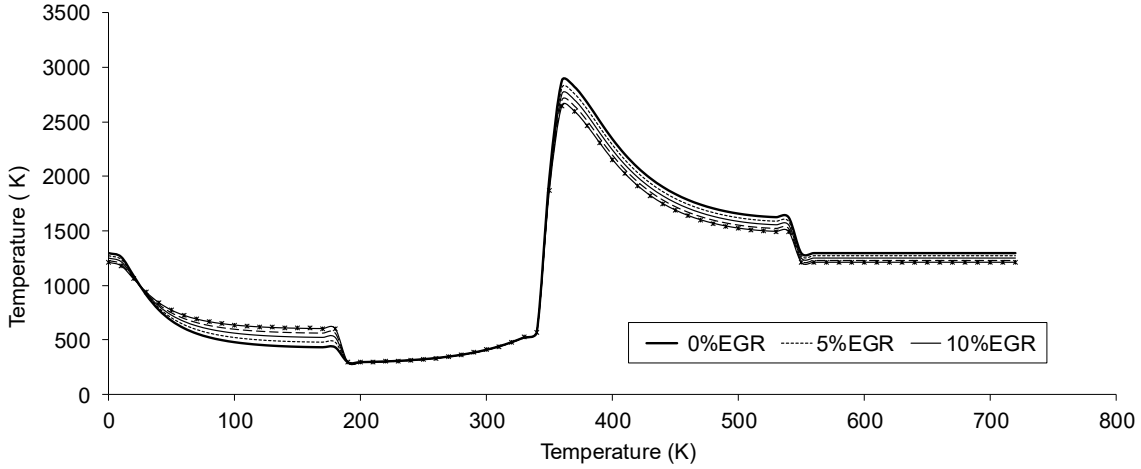

Fig. 11. Indicated temperatures Vs. Degree crank angles of an S.I. engine at 0%, 5%, 10%, 15% and 20% recycled exhaust gas (%EGR)

5.1 Effect of %EGR on simulated indicated work

Figure 12 shows that the indicated work varies inversely with the %EGR. This means that there is a reduction in the net work done by the engine as the recycled exhaust gas increases. From the result of the simulation, the indicated work falls from 0.393kJ at 0%EGR to 0.353 kJ at 20%EGR. This explains why application of EGR gas is a disadvantage when the engine is required to give its maximum work output. Figure 9 shows that the indicated P-V diagram is affected by %EGR. Here the expansion stroke curve bulges inward indicating reduction in the area under the P-V diagram.

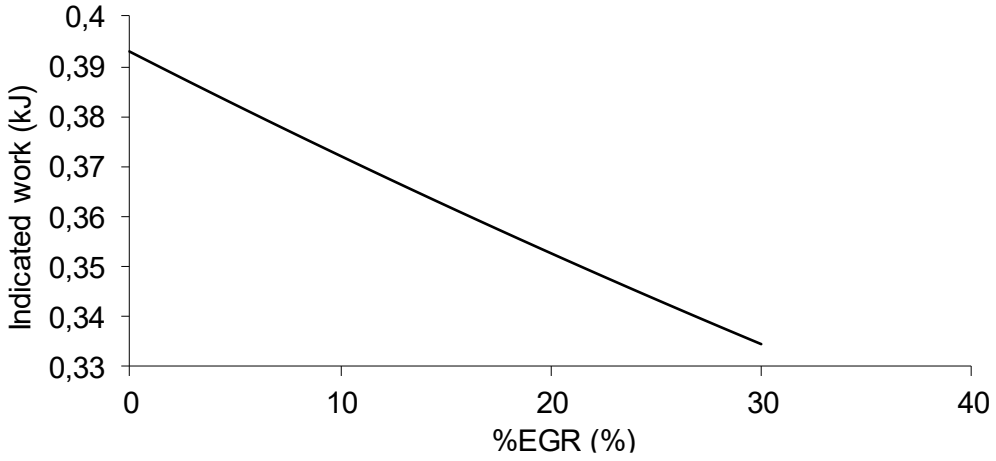

Fig. 12. Simulated indicated work vs. %EGR of an S.I. engine

5.2 Effect of %EGR on indicated power

Similar to the effect of %EGR on Indicated work, Figure 13 shows an inverse variation between the indicated power and %EGR. The indicated power at 0%EGR was 5.895KW, which reduced to 5.290KW at 20%EGR.

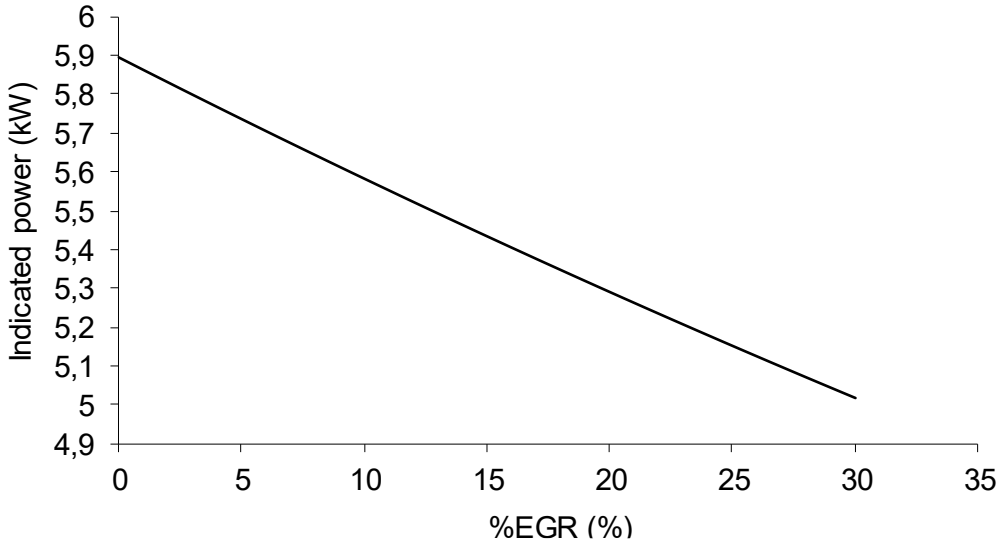

Fig. 13. Simulated indicated power versus %EGR of an S.I. engine

5.3 Effect of %EGR on indicated peak pressure

Figure 14 shows an inverse variation between the cylinder peak pressure and %EGR. At 0%EGR, (i.e. without introduction of recycled exhaust gas), the cylinder peak pressure was determined to be 5681 kPa. At 20%EGR, the cylinder peak pressure dropped to 5228 kPa. That is a significant reduction of 453kPa. This relationship between %EGR and cylinder peak pressure is the basis for the use of EGR as a means of emission control. NO_x concentration has been observed to reduce with a reduction in the cylinder peak pressure [23]. Figure 10 also

shows the effect of %EGR on Cylinder Peak Pressure; on the graph of Indicated Pressure versus degree crank angles for 0%, 5%, 10%, 15%, and 20% EGR.

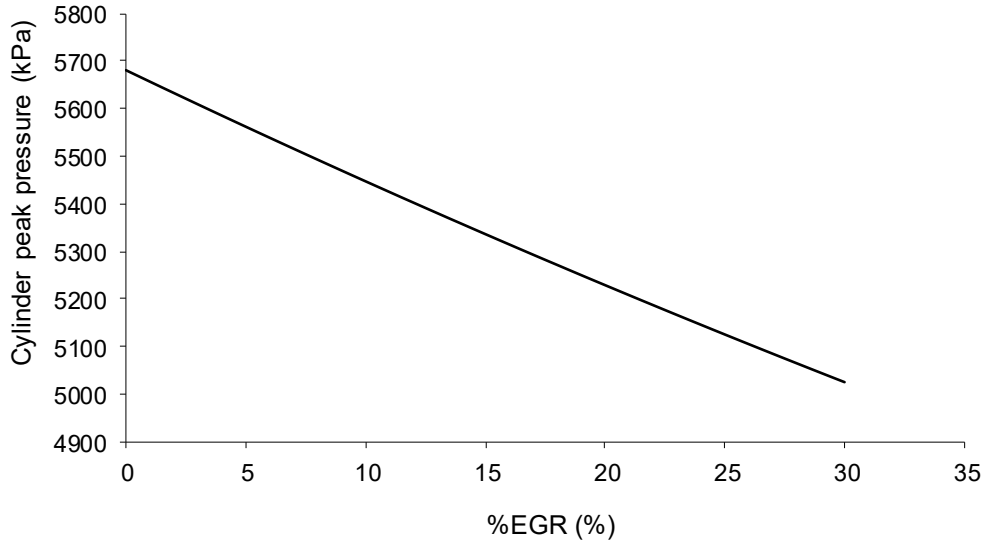

Fig. 14. Simulated cylinder peak pressure vs. %EGR of an S.I. engine

5.4 Effect of %EGR on cylinder peak temperature

Similar to the effect of %EGR on Cylinder Peak Pressure discussed above, Figure 15 shows that the Cylinder Peak temperature varies inversely with %EGR. The simulated results show a variation from 2877K at 0%EGR to 2647K at 20%EGR. This means a reduction of 230K in the cylinder peak temperature was achieved by the application of up to 20%EGR. This relationship forms the basis for the use of the EGR system to control the emission of NO_x, which varies largely with cylinder peak temperature [24]. Figure 11 also shows the effect of %EGR on cylinder peak temperature, on the graph of Indicated Temperature versus degree crank angles for 0%, 5%, 10%, 15%, and 20% EGR.

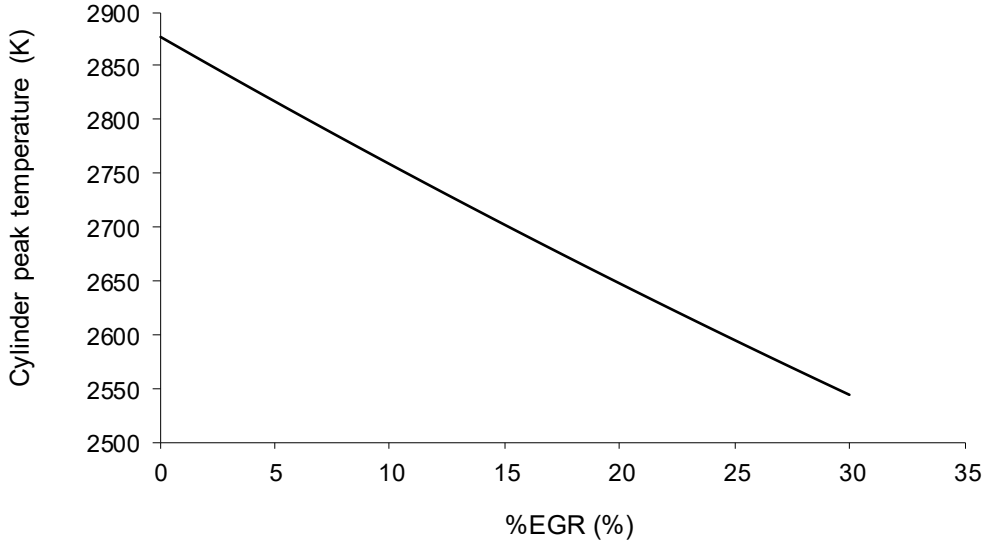

Fig. 15. Simulated cylinder peak temperature vs. %EGR of an S.I. engine

5.5 Effect of% EGR on indicated mean effective pressure

The Indicated mean effective pressure (P_{imep}) is an important engine parameter. Figure 16 shows that P_{imep} is inversely proportional to %EGR. The results of the Simulation show that P_{imep} at 0%EGR was calculated to be 641 kPa, and reduces to 576 kPa at 20%EGR.

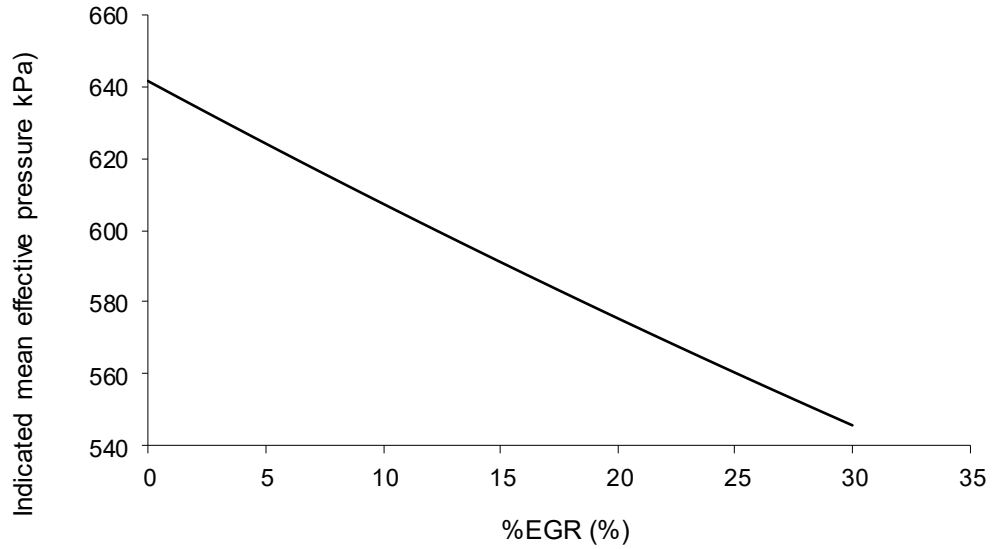

Fig. 16. Simulated mean effective pressure vs. %EGR of an S.I. engine

5.6 Effect of%EGR on indicated thermal efficiency

Figure 17 shows the correlation between %EGR and indicated thermal efficiency. It also shows that the indicated thermal efficiency varies almost directly with the %EGR. The results in Table 5 show a slight increase in thermal efficiency with respect to %EGR. The thermal efficiency for 0%EGR was determined to be 20.73% while at 20%EGR the thermal efficiency was 23.32%. This shows an increase in the indicated thermal efficiency by 2.59% for the application of 20% EGR.

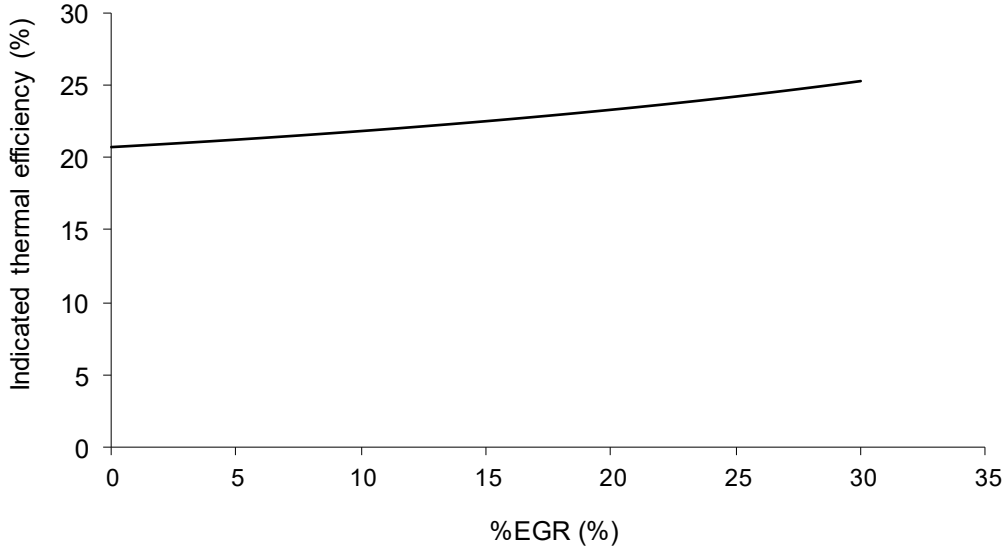

Fig. 17. Indicated thermal eficiency vs. %EGR of an S.I. engine

5.7 Effect of%EGR on residual fraction

Figure 18 shows that the residual fraction varies directly with the%EGR. The simulated results show that the residual fraction varies from 0.058 at 0%EGR to 0.062 at 20%EGR. That is an increase of 0.004 residual fraction due to the application of 20% EGR.

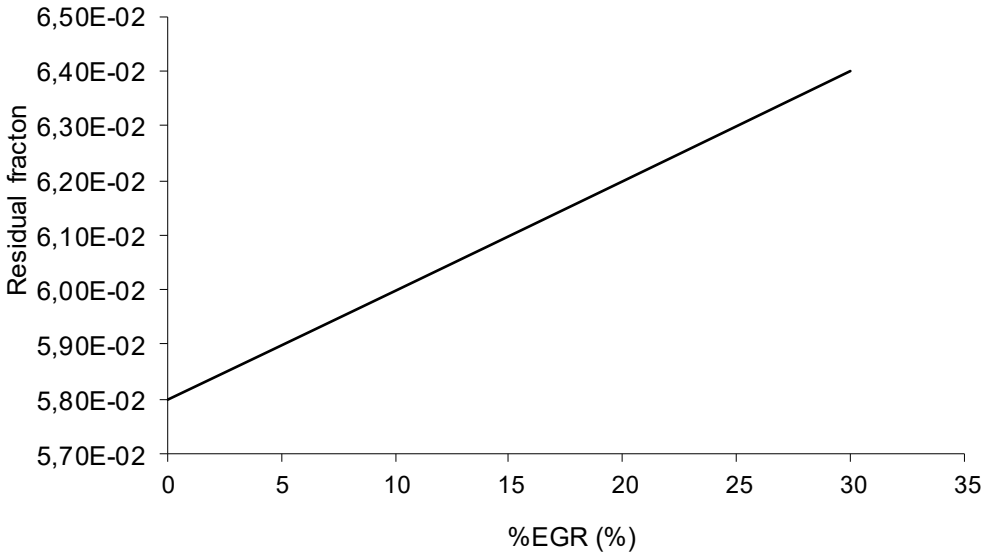

Fig. 18. Residual fraction vs. %EGR of an S.I. engine

5.8 Effect of%EGR on heat released rate

The Blumberg model was used for the heat released rate. The model assumes that the fuel burns according to a trigonometric relationship. Figure 19 shows the relation between the heat released ratio and crank angle ratio for 0%EGR. Figure 24 shows the relationship between the heat released rate and the crank angle ratio for 0% EGR. Figure 25 shows the relationship between the heat released rate and the crank angle ratio for 0%, 5%, 10%, 15%, and 20% EGR. It can be easily seen from figure 24 that as the %EGR increases, the maximum value of the heat released rate reduces [25]. This also explains the reason for the reduction in the peak pressure and temperature.

5.9 Recycled exhaust gas (EGR) velocity

The recycled exhaust gas velocity (EGR velocity) depends on the upstream and downstream pressure of the EGR valve and the specific heat ratio of the recycled exhaust gas. A coefficient of discharge of 0.95 was assumed for the EGR valve to take care of possible losses. The result of the simulation for an inlet temperature of 400K, upstream and downstream pressures of 105 kPa and 95 kPa respectively, gives a subsonic velocity of 3.802m/s for the recycled exhaust gas. The velocity is constant for a given upstream and downstream pressure. The result is as shown in Figure 20. For a supercharged S.I. engine, the EGR gas velocity varies with the pressure, that is, the pressure at which the recycled exhaust gas is pumped into the valve. This is clearly shown in Figure 20.

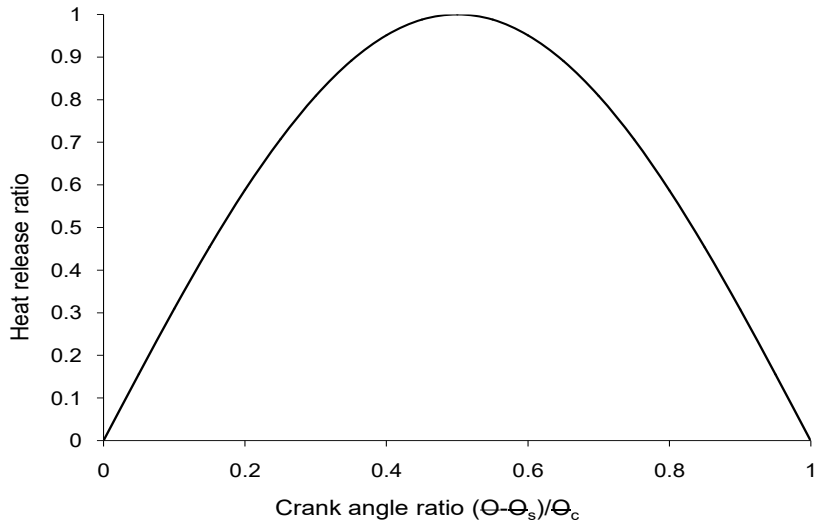

Fig. 19. Heat released ratio vs. crank angle ratio for an SI engine at 0%EGR

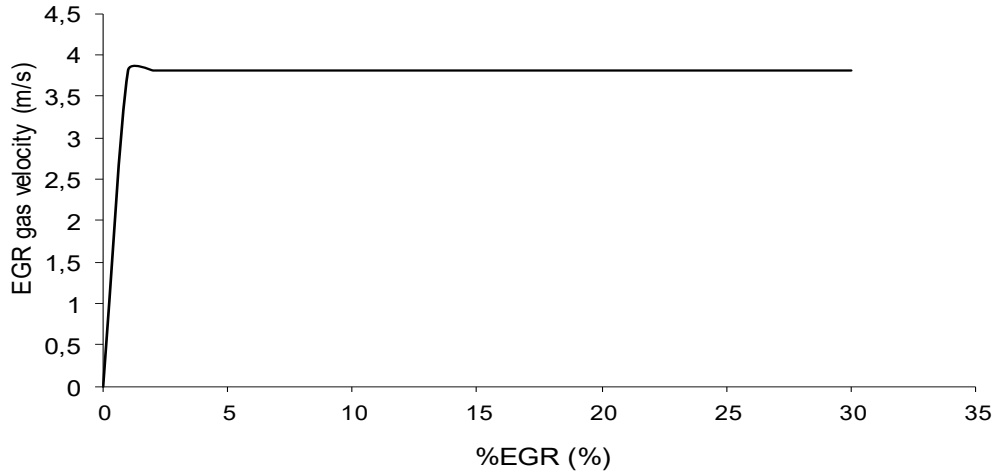

Fig. 20. EGR gas downstream velocity Vs. %EGR for an S.I. engine

5.10 Recycled gas mass flow rate and the EGR valve lift

The EGR mass flow rate is a measure of the quantity of the recycled exhaust gas that flows into the cylinder. The quantity of recycled exhaust gas (EGR) that is allowed to dilute the intake charge can be varied with the aid of the valve lift. The valve lift is therefore the parameter used in controlling the quantity of the recycled exhaust gas that is allowed to dilute the air-fuel mixture. Using the valve shown in Figure 4 as a case study, the valve lift regulates the cross-sectional area through which the EGR gas flows within the pintle valve; and consequently, the quantity that is allowed per unit time. Figures 21 and 22 show that the valve lift can be used to

vary the%EGR. For the particular EGR pintle valve specification, the valve lift varies from 0-4.64mm for 0 to 18%EGR gas.

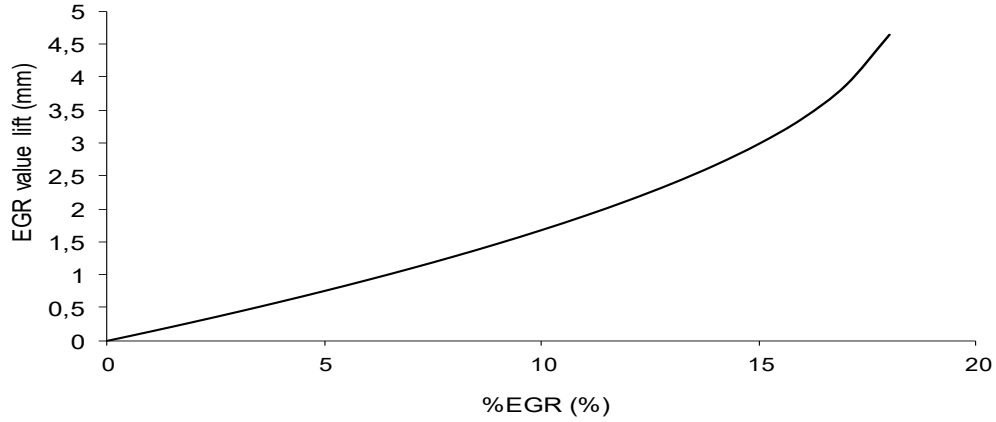

Fig. 21. EGR valve lift vs. %EGR for an S.I. engine

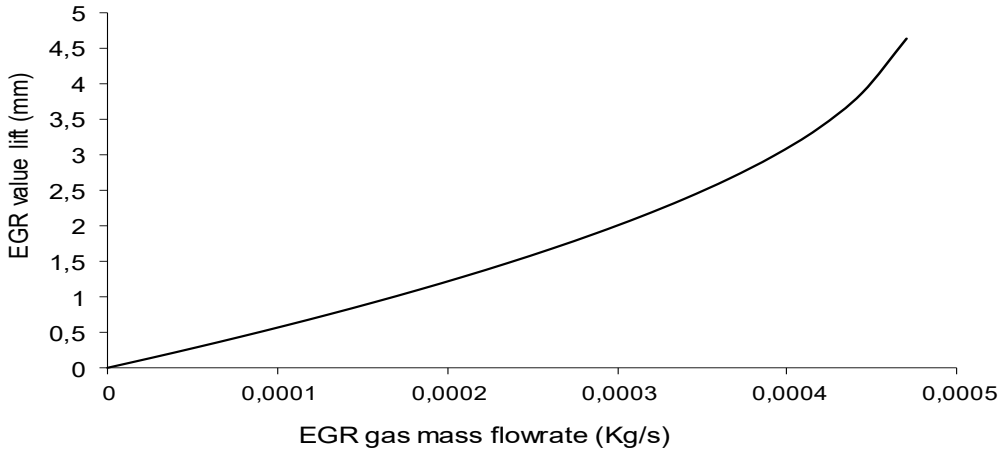

Fig. 22. EGR valve lift vs. EGR gas mass flow rate for an S.I. engine

5.11 Specific heat ratio and%EGR

The basis for the use of EGR system for NO_x emission control was already discussed in detail under the literature review of this report. The result of our simulation shows that the Cylinder Peak Temperature decreases with an increase of%EGR. It was already established that the value of the specific heat ratio of the in-cylinder charge reduces with an increase in the %EGR. This is caused by an increase in the heat capacity of the in-cylinder gas and the retardation of ignition timing is an effect. For the simulation, a hypothetical variation (estimated values) of the specific heat ratio, γ, for the combustion process was made from the following exponential equation, which allows γ to vary from 1.25 for 0% EGR to lower values of γ as %EGR increases (Figure 23).

$$\gamma = 1.25e^{(\%EGR/-450)} \tag{57}$$

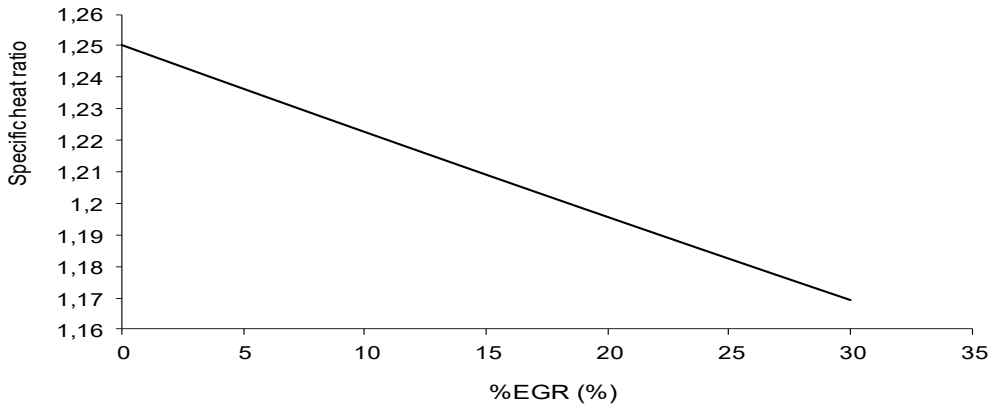

Fig. 23. Estimated specific heat ratio vs. % EGR of the in-cylinder gas during the combustion process for and S.I. engine

Moreover, the Heat released rate Vs. crank angle ratio are shown in Figures 24 and 25.

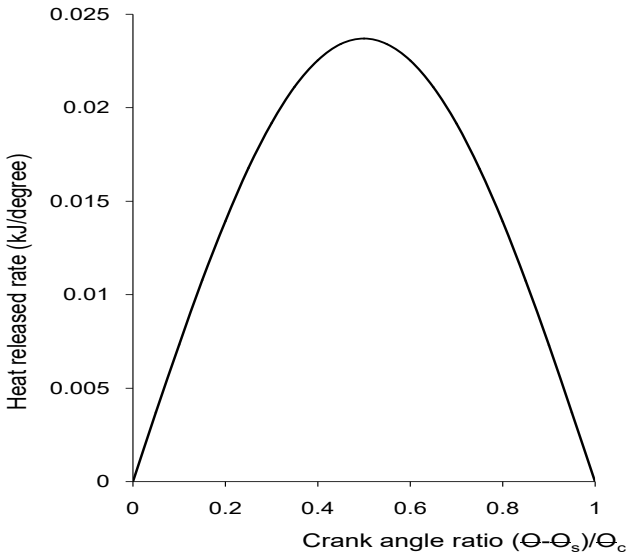

Fig. 24. Heat released rate vs. crank angle ratio for an SI engine at 0%EGR

6. CONCLUSIONS

In conclusion, it has been shown from the results of the simulation that the effective application of EGR in emission control of SI engine should be a compromise between some operating conditions and performance parameters such that:

1. The effective mean pressure and indicated thermal efficiency are not reduced below acceptable levels.
2. The combustion temperature is substantially reduced in order to reduce NOx, while achieving condition 1 above [22].

3. The applied quantity of the diluent EGR gas does not affect the smooth operation of the engine at various operating conditions.
4. While attempting to substantially reduce production of NOx pollutants, concentrations of other pollutants like HC and CO are equally reduced.

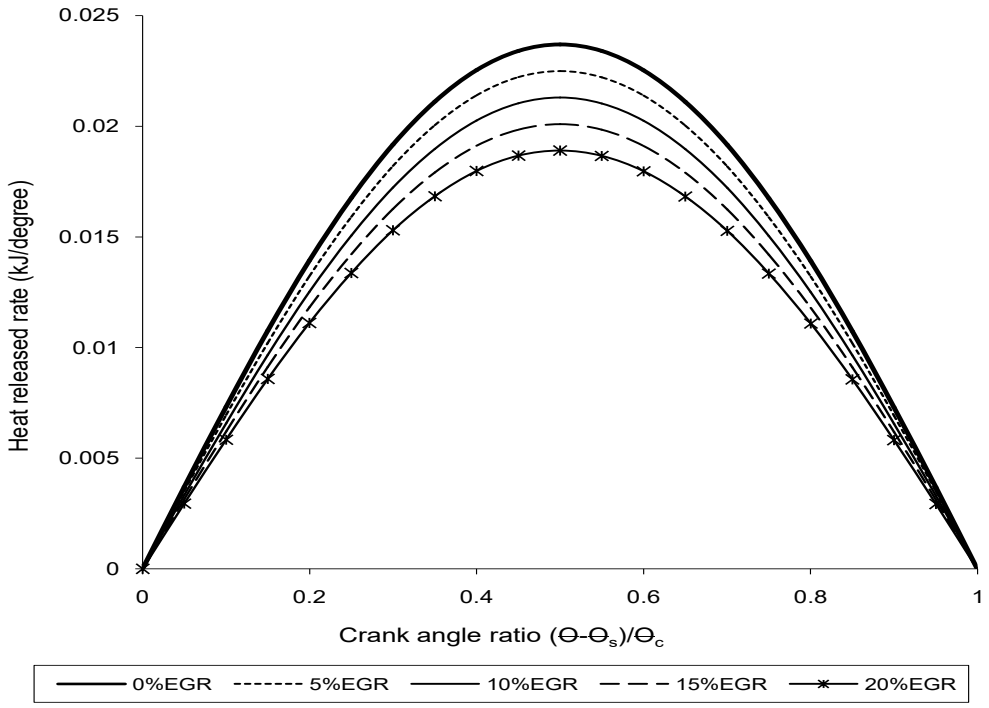

Fig. 25. Heat released rate vs. crank angle ratio for an SI engine at 0-20%EGR

An important aspect of the work is to reduce NOx emissions, a required amount of the recycled exhaust gas (EGR gas) is added to the intake charge so as to keep the peak cycle temperature to a minimum level. This has a great influence on the results. The determination of the EGR valve lift depends on the required value of %EGR for optimum emission control. The EGR valve lift, of course is a function of %EGR, Specific heat ratio of the recycled exhaust gas, γ, mass flow rate of the air-fuel mixture, M_{afN}, and the Pressure, P_e, and Temperature, T_e, of the EGR gas at the inlet of the EGR valve. This implies that there must be an electronic control unit which receives signals from the EGR sensing unit, M_{afN} sensing unit, P_e sensing unit, T_e sensing unit, and compares the same with mapped data, and finally determines the optimum position for the EGR valve.

List of symbols:

Q Heat transfer (kJ)
V Total volume (m^3)
m Total mass (kg)
H Heat transfer coefficient (kJ/m^2 deg)
Q_{app} Apparent heat transfer from combustion (kJ)
T_{wall} Combustion chamber wall Temperature (^oK)
A Area (m^2)
P Pressure (kPa)

γ	Specific heat ratio
LHV	Lower heating value (kJ/kg)
FA	Fuel / Air ratio (kg/kg)
AF	Air / Fuel ratio (kg/kg)
θ	Crank angle degree (degrees)
S	Stroke (m)
S_p	Mean piston speed (m/s)
T	Temperature (^oK)
N	Engine speed (rev/min)
B	Cylinder bore (m)
V_c	Clearance volume (m^3)
x	Piston displacement from (TDC) (m)
V_{444}	Volume of products expanded to exhaust pressure (m^3)
V_s	Swept volume (m^3)
V_t	Cylinder Total volume (m^3)
P_4	Pressure at the end of expansion before valve opening (kPa)
P_{e1}	Pressure of Recycled exhaust gas at the inlet of the EGR valve (kPa)
T_1	Temperature at the start of the intake stroke (^oK)
T_{int}	Temperature of the intake charge (intake manifold temperature) (^oK)
T_{44}	Temperature of product expanded to intake pressure (^oK)
P_{int}	Pressure of the intake charge (intake manifold pressure) (kPa)
T_4	Temperature at the end of expansion before valve opening (^oK)
T_{pk}	Estimated temperature of combustion process (^oK)
T_{all}	Permissible limit of combustion temperature for optimum emission control (^oK)
X_t	Throttle position
η_v	Volumetric efficiency
η_i	Indicated Thermal efficiency
ρ	Density (kg/m^3)
u	Velocity (m/s)
ν	Specific volume (m^3/kg)
Ma	Mach number
c	Local velocity of sound in the fluid (m/s)
M_{afN}	Throttle or Air – Fuel mixture mass flow rate (kg/s)
M_{eN}	Mass flow rate of exhaust gas through the EGR valve (kg/s)
M_{afre}	Mass of (air + fuel + residual gas + recycled exhaust gas) in the cylinder (kg)
M_{af}	Mass of air-fuel mixture in the cylinder (kg)
M_r	Mass of residual gas in the cylinder (kg)
M_e	Mass of recycled exhaust gas in the cylinder (kg)
M_f	Mass of fuel in the cylinder (kg)
θ_o	Crank angle degree at start of the combustion process (degrees)
θ_c	Combustion process duration in Crank angle degree (degrees)
CR	Compression ratio
r	Crank length (m)
l	Connecting rod length (m)
V_θ	Cylinder volume at any degree crank angle, θ. (m^3)
T_θ	Cylinder Temperature at any degree crank angle, θ. (^oK)
P_θ	Cylinder Pressure at any degree crank angle, θ. (kPa)

References

1. Aderibigbe A.A., A.D. Ogunsola, E.A. Fadiji, O. Adeyi, A.J. Adeyi, E.A. Owoo. 2025. "Performance Prediction for Spark Ignition Engines Using Artificial Neural Networks: Model Design And Validation". *Asian Journal of Advanced Research and Reports* 19(1): 201-212. DOI: https://doi.org/10.9734/ajarr/2025/v19i1874.
2. Lee Jeongwoo, Sanghyun Chu, Insuk Ko, Jaegu Kang, Hyunsung Jung, Yohan Chi, Kyoungdoug Min. 2024."Effects Of Dual-Spark Ignition System With Two Different Piston Bowl Shapes On Combustion And Efficiency In A Single-Cylinder Engine". *International Journal of Engine Research* 26(2). DOI: https://doi.org/10.1177/14680874241272886
3. Paluch Maciej, Marcin Noga. 2025. "Influence Of Hydrogen Addition On Performance And Ecological Parameters Of A Spark-Ignition Internal Combustion Engine at Part Load Typical For Urban Traffic". *Advances in Science and Technology Research Journal* 19(3): 262-270. DOI: https://doi.org/10.12913/22998624/199738.
4. Quader Ather A. 1971. "Why Intake Charge Dilution Decreases Nitric Oxide Emission from Spark-Ignition Engines". *SAE Paper* 710009, SAE Transactions 80. Available at: https://www.jstor.org/stable/44731349.
5. Tahtouh Toni, Mathieu André, Giuseppe Castellano, Luciano Rolando, Federico Millo. 2025. "A Path Toward A New Generation Of Sustainable Spark Ignition Engines: Experimental In Investigations On The Synergic Use Of Dual Diluted Combustion And Renewable Fuels". *Transportation Engineering* 20(100317). DOI: https://doi.org/10.1016/j.treng.2025.100317.
6. Agu Hillary. 2025. "Rehabilitation And Upgrade For The Configuration Techniques Of A Spark Ignition Engine Test Bed: A Case Study Of Caritas University Amorji Nik Emene Enugu". *Caritas Journal of Engineering Technology* 4(1): 64-75.
7. Duan Xiongbo, Lubin Xu, Linxun Xu, Pengfei Jiang, Tian Gan, Haibo Liu, Shaobo Ye, Zhiqiang Sun. 2023. "Performance Analysis and Comparison of the Spark Ignition Engine Fuelled with Industrial By-Product Hydrogen and Gasoline". *Journal of Cleaner Production* 424(20). Article 138899. DOI: https://doi.org/10.1016/j.jclepro.2023.138899.
8. Assad Mohamad, V.V. Pisarev, A.N. Oznobishin. 2025. "Polycyclic Aromatic Hydrocarbons In Emissions Of The Internal Combustion Spark-Ignition Engine". *Journal of Engineering Physics and Thermophysics* 98: 362-372. DOI: https://doi.org/10.1007/s10891-025-03110-5.
9. Elkelawy Medhat, E.A. El Shenawy, Hagar Alm-Eldin Bastawissi, Emad Mostafa. 2025. "Experimental Investigation on the Effect of Using Gasoline with Commercial Additives on Spark Ignition Engines Performance And Emissions Characteristic". *Journal of Engineering Research* 9(2). Article 8. DOI: https://doi.org/10.70259/engJER.2025.921942.
10. Sforza Lorenzo, Federico Ramognino, Tarcisio Cerri, Giovanni Gaetano Gianetti, Gianluca D'Errico, Angelo Onorati, Josep Gomez-Soriano, Ricardo Novella. 2025. "A 1D-3D Numerical Study Of A Pent-Roof Spark-Ignition Engine Fueled With Hydrogen Lean Mixtures". *International Journal of Engine Research*. DOI: https://doi.org/10.1177/14680874251355646.

11. Aderibigbe A.A., A.D. Ogunsola, E.A. Fadiji, E.A. Owoo, O. Adeyi, A.J. Adeyi, M.A. Olojede. 2024. "Theoretical Analysis Of Performance Characteristics Of Non- Road Spark Ignition Engines". *Journal of Energy Research and Reviews* 16(12): 47-60. DOI: https://doi.org/10.9734/jenrr/2024/v16i12386.
12. Sorenson S.C. 1981. "Simple Computer Simulations For Internal Combustion Engine Instruction". *Internal Journal of Mechnaical Engineering* 9(3): 237-243.
13. Ryder G.H. M.D. Bennett. 1975. *Mechanics of Machines*. Macmillan Education Ltd., Houndmills, Basingstroke, Hants R G21 2xs.
14. Ferguson Colin R., Allan T. Kirkpatrick. *Applied Thermosciences*. 2016. John Wiley & Sons Ltd, West Sussex, PO19 8SQ, United Kingdom.
15. Akar Şule, Emre Arabacı. 2025. "Effects of Valve Overlap, Lift, and Duration on Spark Ignition Engine Performance". *International Journal of Automotive Science And Technology* 9(2): 218-229. DOI: https://doi.org/10.30939/ijastech..1655212.
16. Douglas J.M. Gasiorek, J.A. Swaffield, Lynne B. Jack. 1985. *Fluid Mechanics*. 2nd Edition, Longman Scientific and Technical, Longman Group UK Ltd, Longman House, Burnt Mill, Harlow, Essex CM20 2JE, England.
17. Binder Raymond Charles. 1958. *Advanced Fluid Mechanics*. Volume II, Prentice-Hall, Incorporated, Englewood Cliffs, N.J.
18. Kao Minghui, John J. Moskwa. 1995. "Turbocharged Diesel Engine Modeling for Nonlinear Engine Control and State Estimation". *Journal of Dynamic Systems, Measurement, and Control, Transactions of the ASME* 117: 20-30. DOI: https://doi.org/10.1115/1.2798519.
19. Champion R.C., E.C. Arnold. 1970. *Motor Vehicle Calculations and Science*. Part 2. S.I. Units, Edward Arnold Publishers, Limited 441 Bedford Square, London, WC1B 3DQ.
20. Rogers Gordon, Yon Mayhew. 2002. *Engineering Thermodynamics Work and Heat Transfer*. 4th Edition S.I. Units, English Language Book Society and Longman.
21. Komiyama Kunihiko, John B. Heywood. 1973. "Predicting NOx Emissions and Effects of Exhaust Gas Recirculation in Spark-Ignition Engines". *SAE Paper* 730475, SAE Transaction 82. Available at: https://www.jstor.org/stable/44717557.
22. Blumberg Paul, J.T. Kummer. 1971. "Prediction of NO formation in Spark-Ignition Engines – An Analysis of methods of control". *Combustion Science Technology* 4: 73-96. DOI: https://doi.org/10.1080/00102207108952474.
23. Lavoie George A., John B. Heywood, James C. Keck 1970. "Experimental and Theoretical Investigation of Nitric Oxide Formation in Internal Combustion Engines". *Combustion Science Technology* 1: 313-326. DOI: https://doi.org/10.1080/00102206908952211.
24. Hilliard John C., Richard W. Wheeler. 1979. "Nitrogen Dioxide in Engine Exhaust". *SAE Paper* 790691, SAE Transaction 88. Available at: https://www.jstor.org/stable/44699062.
25. Borman Gary, Kazuie Nishiwaki. 1987. "A Review of International Combustion Engine Heat transfer". *Progress in Energy and Combustion Science* 13: 1-46. DOI: https://doi.org/10.1016/0360-1285(87)90005-0.

Received 26.09.2025; accepted in revised form 25.02.2026